Radial basis functions for neutron transport: theory manual

Brody Bassett

December 2, 2016

Contents

Part I
Discretization of the neutron transport equation

1 Introduction to transport equation

Variable	Description	Units
$\boldsymbol{x}$	Position	cm
E	Energy	MeV
$\boldsymbol{\Omega}$	Direction	steradian^{-1}
t	Time	s
$\psi(\boldsymbol{x}, \boldsymbol{\Omega}, E, t)$	Angular flux at position $\boldsymbol{x}$ in direction $\boldsymbol{\Omega}$ with energy E	particles cm^{-2} s^{-1} MeV^{-1} steradian^{-1}
$\phi_\ell^m(\boldsymbol{x}, E, t)$	Spherical harmonic moment of the angular flux of degree ℓ and order m	particles cm^{-2} s^{-1} MeV^{-1}
$v(E)$	Particle speed	cm s^{-1}
$\Sigma_t(\boldsymbol{x}, E)$	Total cross section at position $\boldsymbol{x}$ for particles with energy E	cm^{-1}
$\Sigma_s(\boldsymbol{x}, \boldsymbol{\Omega}' \cdot \boldsymbol{\Omega}, E' \to E)$	Scattering cross section at position $\boldsymbol{x}$ for particles scattering from direction $\boldsymbol{\Omega}'$ to $\boldsymbol{\Omega}$ and from energy E' to E	MeV^{-1}
$\chi(\boldsymbol{x}, E)$	Fission spectrum for energy E for fissions occurring at position $\boldsymbol{x}$	MeV^{-1}
$\nu(\boldsymbol{x}, E)$	Average number of neutrons created in a fission for a neutron at position $\boldsymbol{x}$ and with energy E	particles
$\Sigma_f(\boldsymbol{x}, E)$	Fission cross section at position $\boldsymbol{x}$ for particles of energy E	cm^{-1}
$q(\boldsymbol{x}, \boldsymbol{\Omega}, E, t)$	Internal particle source at position $\boldsymbol{x}$ in direction $\boldsymbol{\Omega}$ with energy E	particles cm^{-3} s^{-1} MeV^{-1}

Table 1: Variables in the transport equation

1.1 Continuous transport equation

Begin with the neutron transport equation without delayed neutrons,

$$\begin{aligned}\frac{1}{v(E)}\frac{\partial}{\partial t}\psi(\boldsymbol{x}, \boldsymbol{\Omega}, E, t) + \boldsymbol{\Omega} \cdot \boldsymbol{\nabla}\psi(\boldsymbol{x}, \boldsymbol{\Omega}, E, t) + \Sigma_t(\boldsymbol{x}, E)\,\psi(\boldsymbol{x}, \boldsymbol{\Omega}, E, t) \\ = \int_0^\infty \int_{4\pi} \Sigma_s(\boldsymbol{x}, \boldsymbol{\Omega}' \cdot \boldsymbol{\Omega}, E' \to E)\,\psi(\boldsymbol{x}, \boldsymbol{\Omega}', E', t)\,d\Omega' dE' \\ + \chi(\boldsymbol{x}, E) \int_0^\infty \int_{4\pi} \nu(\boldsymbol{x}, E')\,\Sigma_f(\boldsymbol{x}, E')\,\psi(\boldsymbol{x}, \boldsymbol{\Omega}', E', t)\,d\Omega' dE' + q(\boldsymbol{x}, \boldsymbol{\Omega}, E, t), \\ \boldsymbol{x} \in V, \quad \boldsymbol{\Omega} \in 4\pi, \quad 0 < E < \infty, \quad 0 < t, \quad (1)\end{aligned}$$

and the accompanying boundary and initial conditions,

$$\psi(\boldsymbol{x}, \boldsymbol{\Omega}, E, t) = \psi^b(\boldsymbol{x}, \boldsymbol{\Omega}, E, t) + \rho\psi(\boldsymbol{x}, \boldsymbol{\Omega}_r, E, t), \qquad \boldsymbol{x} \in V, \quad \boldsymbol{\Omega} \cdot \boldsymbol{n} < 0, \quad 0 < E < \infty, \quad 0 < t, \quad (2)$$

$$\psi(\boldsymbol{x}, \boldsymbol{\Omega}, E, t=0) = \psi^i(\boldsymbol{x}, \boldsymbol{\Omega}, E), \qquad \boldsymbol{x} \in V, \quad \boldsymbol{\Omega} \in 4\pi, \quad 0 < E < \infty. \tag{3}$$

Here ρ allows for the albedo boundary condition with $\rho = 1$ for a reflective boundary condition and $\rho = 0$ for a vacuum boundary condition. The reflection angle is $\boldsymbol{\Omega}_r = \boldsymbol{\Omega} - 2(\boldsymbol{\Omega} \cdot \boldsymbol{n})\boldsymbol{n}$. Defining the spherical harmonics moments of the equation as

$$\phi_\ell^m(\boldsymbol{x}, E, t) \equiv \int_{4\pi} Y_\ell^m(\boldsymbol{\Omega}) \psi(\boldsymbol{x}, \boldsymbol{\Omega}, E, t) \, d\Omega, \tag{4}$$

and using a similar expression for the representation of the scattering source,

$$\Sigma_{s;\ell}(\boldsymbol{x}, E' \to E) \equiv 2\pi \int_{-1}^{1} P_\ell(\mu_0) \Sigma_s(\boldsymbol{x}, \mu_0, E' \to E) \, d\mu_0 \tag{5}$$

(with the scattering cosine $\mu_0 = \boldsymbol{\Omega}' \cdot \boldsymbol{\Omega}$), we get the approximations

$$\psi(\boldsymbol{x}, \boldsymbol{\Omega}, E, t) = \sum_{\ell=0}^{\infty} \frac{2\ell+1}{4\pi} \sum_{m=-\ell}^{\ell} Y_\ell^m(\boldsymbol{\Omega}) \phi_\ell^m(\boldsymbol{x}, E, t), \tag{6}$$

$$\Sigma_s(\boldsymbol{x}, \boldsymbol{\Omega}' \cdot \boldsymbol{\Omega}, E' \to E) = \sum_{\ell=0}^{\infty} \sum_{m=-\ell}^{\ell} \Sigma_{s,\ell}(\boldsymbol{x}, E) Y_\ell^m(\boldsymbol{\Omega}) Y_\ell^m(\boldsymbol{\Omega}') \tag{7}$$

(where we have assumed that the Y_ℓ^m are the real spherical harmonic moments). Applying these simplifications to the scattering and fission terms gives

$$\begin{aligned} &\frac{1}{v(E)} \frac{\partial}{\partial t} \psi(\boldsymbol{x}, \boldsymbol{\Omega}, E, t) + \boldsymbol{\Omega} \cdot \boldsymbol{\nabla} \psi(\boldsymbol{x}, \boldsymbol{\Omega}, E, t) + \Sigma_t(\boldsymbol{x}, E) \psi(\boldsymbol{x}, \boldsymbol{\Omega}, E, t) \\ &\qquad = \sum_{\ell=0}^{\infty} \frac{2\ell+1}{4\pi} \sum_{m=-\ell}^{\ell} Y_\ell^m(\boldsymbol{\Omega}) \int_0^\infty \Sigma_{s;\ell}(\boldsymbol{x}, E' \to E) \phi_\ell^m(\boldsymbol{x}, E', t) \, dE' \\ &\qquad + \frac{\chi(\boldsymbol{x}, E)}{4\pi} \int_0^\infty \nu(\boldsymbol{x}, E') \Sigma_f(\boldsymbol{x}, E') \phi_0^0(\boldsymbol{x}, E', t) \, dE' + q(\boldsymbol{x}, \boldsymbol{\Omega}, E, t), \\ &\qquad\qquad \boldsymbol{x} \in V, \quad \boldsymbol{\Omega} \in 4\pi, \quad 0 < E < \infty, \quad 0 < t. \end{aligned} \tag{8}$$

2 Angular, energy and time simplifications to transport equation

2.1 Multigroup transport equation

The multigroup approximation begins with a neutron spectrum approximation, $\Psi(\boldsymbol{x}, E)$, with which each of the energy-dependent cross sections is weighted over an energy range $E \in [E_g, E_{g-1}]$ to get multigroup cross sections, neutron velocities and fission sources,

$$\Sigma_{t;g}(\boldsymbol{x}) \equiv \frac{\int_{E_g}^{E_{g-1}} \Sigma_t(\boldsymbol{x}, E) \Psi(\boldsymbol{x}, E) \, dE}{\int_{E_g}^{E_{g-1}} \Psi(\boldsymbol{x}, E) \, dE}, \tag{9a}$$

$$\Sigma_{s;\ell,g' \to g}(\boldsymbol{x}) \equiv \frac{\int_{E_g}^{E_{g-1}} \int_{E_{g'}}^{E_{g'-1}} \Sigma_{s;\ell}(\boldsymbol{x}, E' \to E) \Psi(\boldsymbol{x}, E') \, dE' dE}{\int_{E_{g'}}^{E_{g'-1}} \Psi(\boldsymbol{x}, E') \, dE'}, \tag{9b}$$

$$\frac{1}{\nu_g(\boldsymbol{x})} \equiv \frac{\int_{E_g}^{E_{g-1}} \frac{1}{v(E)} \Psi(\boldsymbol{x}, E) \, dE}{\int_{E_g}^{E_{g-1}} \Psi(\boldsymbol{x}, E) \, dE}, \tag{9c}$$

$$\nu\Sigma_{f;g}(\boldsymbol{x}) \equiv \frac{\int_{E_g}^{E_{g-1}} \nu(\boldsymbol{x}, E) \Sigma_f(\boldsymbol{x}, E) \Psi(\boldsymbol{x}, E) \, dE}{\int_{E_g}^{E_{g-1}} \Psi(\boldsymbol{x}, E) \, dE}. \tag{9d}$$

The multigroup fission spectrum, angular flux and source are defined as

$$\chi_g(\boldsymbol{x}) \equiv \int_{E_g}^{E_{g-1}} \chi(\boldsymbol{x}, E)\, dE, \tag{9e}$$

$$\psi_g(\boldsymbol{x}, \boldsymbol{\Omega}, t) \equiv \int_{E_g}^{E_{g-1}} \psi(\boldsymbol{x}, \boldsymbol{\Omega}, E, t)\, dE, \tag{9f}$$

$$q(\boldsymbol{x}, \boldsymbol{\Omega}, t) \equiv \int_{E_g}^{E_{g-1}} q(\boldsymbol{x}, \boldsymbol{\Omega}, E, t)\, dE. \tag{9g}$$

Integrate the transport equation over $E \in [E_g, E_{g-1}]$,

$$\begin{aligned}
&\frac{\partial}{\partial t}\int_{E_g}^{E_{g-1}} \frac{1}{v(E)}\psi(\boldsymbol{x}, \boldsymbol{\Omega}, E, t)\, dE + \boldsymbol{\Omega}\cdot\boldsymbol{\nabla}\int_{E_g}^{E_{g-1}} \psi(\boldsymbol{x}, \boldsymbol{\Omega}, E, t)\, dE + \int_{E_g}^{E_{g-1}} \Sigma_t(\boldsymbol{x}, E)\,\psi(\boldsymbol{x}, \boldsymbol{\Omega}, E, t)\, dE \\
&\qquad = \sum_{\ell=0}^{\infty}\frac{2\ell+1}{4\pi}\sum_{m=-\ell}^{\ell} Y_\ell^m(\boldsymbol{\Omega})\int_{E_g}^{E_{g-1}}\int_0^{\infty} \Sigma_{s;\ell}(\boldsymbol{x}, E'\to E)\,\phi_\ell^m(\boldsymbol{x}, E', t)\, dE' dE \\
&\quad + \int_{E_g}^{E_{g-1}} \frac{\chi(\boldsymbol{x}, E)}{4\pi}\int_0^{\infty} \nu(\boldsymbol{x}, E')\,\Sigma_f(\boldsymbol{x}, E')\,\phi_0^0(\boldsymbol{x}, E', t)\, dE' dE + \int_{E_g}^{E_{g-1}} q(\boldsymbol{x}, \boldsymbol{\Omega}, E, t)\, dE, \\
&\qquad\qquad \boldsymbol{x}\in V, \quad \boldsymbol{\Omega}\in 4\pi, \quad g = 1,\ldots,G, \quad 0 < t.
\end{aligned} \tag{10}$$

If weighted integrals of the physical data over $\psi(\boldsymbol{x}, E)$ are approximately equal to weighted integrals over $\psi(\boldsymbol{x}, \boldsymbol{\Omega}, E, t)$ (e.g. for Σ_t,

$$\frac{\int_{E_g}^{E_{g-1}} \Sigma_t(\boldsymbol{x}, E)\,\Psi(\boldsymbol{x}, E)\, dE}{\int_{E_g}^{E_{g-1}} \Psi(\boldsymbol{x}, E)\, dE} \approx \frac{\int_{E_g}^{E_{g-1}} \Sigma_t(\boldsymbol{x}, E)\,\psi(\boldsymbol{x}, \boldsymbol{\Omega}, E, t)\, dE}{\int_{E_g}^{E_{g-1}} \psi(\boldsymbol{x}, \boldsymbol{\Omega}, E, t)\, dE} \tag{11}$$

must hold), the transport equation can be simplified to

$$\begin{aligned}
&\frac{1}{v_g(\boldsymbol{x})}\frac{\partial}{\partial t}\psi_g(\boldsymbol{x}, \boldsymbol{\Omega}, t)\, dE + \boldsymbol{\Omega}\cdot\boldsymbol{\nabla}\psi_g(\boldsymbol{x}, \boldsymbol{\Omega}, t) + \Sigma_{t;g}(\boldsymbol{x})\,\psi_g(\boldsymbol{x}, \boldsymbol{\Omega}, t) \\
&\qquad = \sum_{\ell=0}^{\infty}\frac{2\ell+1}{4\pi}\sum_{m=-\ell}^{\ell} Y_\ell^m(\boldsymbol{\Omega})\sum_{g'=1}^{G} \Sigma_{s;\ell,g'\to g}(\boldsymbol{x})\,\phi_{\ell,g'}^m(\boldsymbol{x}, t) \\
&\quad + \frac{\chi_g(\boldsymbol{x})}{4\pi}\sum_{g'=1}^{G} \nu\Sigma_{f;g'}(\boldsymbol{x})\,\phi_{0,g'}^0(\boldsymbol{x}, t) + q_g(\boldsymbol{x}, \boldsymbol{\Omega}, t), \\
&\qquad\qquad \boldsymbol{x}\in V, \quad \boldsymbol{\Omega}\in 4\pi, \quad g = 1,\ldots,G, \quad 0 < t.
\end{aligned} \tag{12}$$

The initial and boundary equations become

$$\psi_g(\boldsymbol{x}, \boldsymbol{\Omega}, t) = \psi_g^b(\boldsymbol{x}, \boldsymbol{\Omega}, t) + \rho\psi_g(\boldsymbol{x}, \boldsymbol{\Omega}_r, t), \qquad \boldsymbol{x}\in V, \quad \boldsymbol{\Omega}\cdot\boldsymbol{n} < 0, \quad g = 1,\ldots,G, \quad 0 < t, \tag{13a}$$

$$\psi_g(\boldsymbol{x}, \boldsymbol{\Omega}, t = 0) = \psi_g^i(\boldsymbol{x}, \boldsymbol{\Omega}), \qquad \boldsymbol{x}\in V, \quad \boldsymbol{\Omega}\in 4\pi, \quad g = 1,\ldots,G, \tag{13b}$$

where the initial and boundary flux have been integrated over each energy group g.

2.2 Discrete ordinates transport equation

The discrete-ordinates approximation solves the transport equation along particular rays (or ordinates). Defining

$$\psi_{n,g}(\boldsymbol{x}, t) \equiv \psi_g(\boldsymbol{x}, \boldsymbol{\Omega}_n, t), \tag{14a}$$

$$q_{n,g}(\boldsymbol{x},t) \equiv q_g(\boldsymbol{x},\boldsymbol{\Omega}_n,t), \tag{14b}$$

for each discrete direction $\boldsymbol{\Omega}_n$, the transport equation becomes

$$\begin{aligned}\frac{1}{v_g(\boldsymbol{x})}\frac{\partial}{\partial t}\psi_{n,g}(\boldsymbol{x},t)\,dE + \boldsymbol{\Omega}_n\cdot\boldsymbol{\nabla}\psi_{n,g}(\boldsymbol{x},t) + \Sigma_{t;g}(\boldsymbol{x})\,\psi_{n,g}(\boldsymbol{x},t)\\ = \sum_{\ell=0}^{\infty}\frac{2\ell+1}{4\pi}\sum_{m=-\ell}^{\ell}Y_\ell^m(\boldsymbol{\Omega}_n)\sum_{g'=1}^{G}\Sigma_{s;\ell,g'\to g}(\boldsymbol{x})\,\phi_{\ell,g'}^m(\boldsymbol{x},t)\\ + \frac{\chi_g(\boldsymbol{x})}{4\pi}\sum_{g'}\nu\Sigma_{f;g'}(\boldsymbol{x})\,\phi_{0,g'}^0(\boldsymbol{x},t) + q_{n,g}(\boldsymbol{x},t),\\ \boldsymbol{x}\in V,\quad n=1,\dots N,\quad g=1,\dots,G,\quad 0<t.\end{aligned} \tag{15}$$

The boundary and initial conditions become

$$\psi_{n,g}(\boldsymbol{x},t) = \psi_{n,g}^b(\boldsymbol{x},t) + \rho\psi_{n_r,g}^b(\boldsymbol{x},t), \qquad \boldsymbol{x}\in V,\quad \boldsymbol{\Omega}_n\cdot\boldsymbol{n}<0,\quad g=1,\dots,G,\quad 0<t, \tag{16a}$$

$$\psi_{n,g}(\boldsymbol{x},t=0) = \psi_{n,g}^i(\boldsymbol{x}), \qquad \boldsymbol{x}\in V,\quad n=1,\dots N,\quad g=1,\dots,G, \tag{16b}$$

To facilitate integration, the directions $\boldsymbol{\Omega}_n$ are chosen as ordinates in a quadrature set which has the property

$$\int_{4\pi} f(\boldsymbol{\Omega})\,d\Omega \approx \sum_{n=1}^{N} w_n f(\boldsymbol{\Omega}_n). \tag{17}$$

The calculation of the spherical harmonics moments then becomes

$$\phi_{\ell,g}^m(\boldsymbol{x},t) \equiv \sum_{n=1}^{N} w_n Y_\ell^m(\boldsymbol{\Omega}_n)\,\psi_{n,g}(\boldsymbol{x},t). \tag{18}$$

2.3 Steady state transport equation

At steady state, the time derivative in the transport equation goes to zero and time dependence is removed elsewhere, giving

$$\begin{aligned}\boldsymbol{\Omega}_n\cdot\boldsymbol{\nabla}\psi_{n,g}(\boldsymbol{x}) + \Sigma_{t;g}(\boldsymbol{x})\,\psi_{n,g}(\boldsymbol{x})\\ = \sum_{\ell=0}^{\infty}\frac{2\ell+1}{4\pi}\sum_{m=-\ell}^{\ell}Y_\ell^m(\boldsymbol{\Omega}_n)\sum_{g'=1}^{G}\Sigma_{s;\ell,g'\to g}(\boldsymbol{x})\,\phi_{\ell,g'}^m(\boldsymbol{x})\\ + \frac{\chi_g(\boldsymbol{x})}{4\pi}\sum_{g'=1}^{G}\nu\Sigma_{f;g'}(\boldsymbol{x})\,\phi_{0,g'}^0(\boldsymbol{x}) + q_{n,g}(\boldsymbol{x}),\\ \boldsymbol{x}\in V,\quad n=1,\dots N,\quad g=1,\dots,G.\end{aligned} \tag{19}$$

The boundary condition simplifies to

$$\psi_{n,g}(\boldsymbol{x}) = \psi_{n,g}^b(\boldsymbol{x}) + \rho\psi_{n_r,g}(\boldsymbol{x}), \qquad \boldsymbol{x}\in V,\quad \boldsymbol{\Omega}_n\cdot\boldsymbol{n}<0,\quad g=1,\dots,G.$$

3 Spatial discretization of the transport equation

3.1 Strong form of the transport equation

The transport equation can be applied directly to a basis for the angular flux,

$$\psi_{n,g}(\boldsymbol{x}) = \sum_{i=1}^{I}\alpha_{i,n,g}b_i(\boldsymbol{x}),$$

to get

$$\sum_{i=1}^{I}\left[\boldsymbol{\Omega}_n\cdot\boldsymbol{\nabla}b_i\left(\boldsymbol{x}\right)+\Sigma_{t;g}\left(\boldsymbol{x}\right)b_i\left(\boldsymbol{x}\right)\right]\alpha_{i,n,g}$$
$$=\sum_{\ell=0}^{\infty}\frac{2\ell+1}{4\pi}\sum_{m=-\ell}^{\ell}Y_\ell^m\left(\boldsymbol{\Omega}_n\right)\sum_{g'=1}^{G}\Sigma_{s;\ell,g'\rightarrow g}\left(\boldsymbol{x}\right)\phi_{\ell,g'}^m\left(\boldsymbol{x}\right)$$
$$+\frac{\chi_g\left(\boldsymbol{x}\right)}{4\pi}\sum_{g'=1}^{G}\nu\Sigma_{f;g'}\left(\boldsymbol{x}\right)\phi_{0,g'}^0\left(\boldsymbol{x}\right)+q_{n,g}\left(\boldsymbol{x}\right),$$
$$\boldsymbol{x}\in V,\quad n=1,\ldots N,\quad g=1,\ldots,G. \quad (20)$$

In the strong form, this equation is enforced chosen points $\boldsymbol{x}_j\in V$ to get

$$\sum_{i=1}^{I}\left[\boldsymbol{\Omega}_n\cdot\boldsymbol{\nabla}b_i\left(\boldsymbol{x}_j\right)+\Sigma_{t;g}\left(\boldsymbol{x}_j\right)b_i\left(\boldsymbol{x}_j\right)\right]\alpha_{i,n,g}$$
$$=\sum_{\ell=0}^{\infty}\frac{2\ell+1}{4\pi}\sum_{m=-\ell}^{\ell}Y_\ell^m\left(\boldsymbol{\Omega}_n\right)\sum_{g'=1}^{G}\Sigma_{s;\ell,g'\rightarrow g}\left(\boldsymbol{x}_j\right)\phi_{\ell,g'}^m\left(\boldsymbol{x}_j\right)$$
$$+\frac{\chi_g\left(\boldsymbol{x}_j\right)}{4\pi}\sum_{g'=1}^{G}\nu\Sigma_{f;g'}\left(\boldsymbol{x}_j\right)\phi_{0,g'}^0\left(\boldsymbol{x}_j\right)+q_{n,g}\left(\boldsymbol{x}_j\right),$$
$$j=1,\ldots,J,\quad n=1,\ldots N,\quad g=1,\ldots,G. \quad (21)$$

3.2 Weak form of the transport equation

Multiply the steady-state transport equation by a series of weight functions $w_j\left(\boldsymbol{x}\right)$ (for $j=1,\ldots,J$) and integrate over the region of support V_j of $w_j\left(\boldsymbol{x}\right)$ to get

$$\int_{V_j}w_j\left(\boldsymbol{x}\right)\boldsymbol{\Omega}_n\cdot\boldsymbol{\nabla}\psi_{n,g}\left(\boldsymbol{x}\right)dV+\int_{V_j}w_j\left(\boldsymbol{x}\right)\Sigma_{t;g}\left(\boldsymbol{x}\right)\psi_{n,g}\left(\boldsymbol{x}\right)dV$$
$$=\sum_{\ell=0}^{\infty}\frac{2\ell+1}{4\pi}\sum_{m=-\ell}^{\ell}Y_\ell^m\left(\boldsymbol{\Omega}_n\right)\sum_{g'=1}^{G}\int_{V_j}w_j\left(\boldsymbol{x}\right)\Sigma_{s;\ell,g'\rightarrow g}\left(\boldsymbol{x}\right)\phi_{\ell,g'}^m\left(\boldsymbol{x}\right)dV$$
$$+\int_{V_j}w_j\left(\boldsymbol{x}\right)\frac{\chi_g\left(\boldsymbol{x}\right)}{4\pi}\sum_{g'=1}^{G}\nu\Sigma_{f;g'}\left(\boldsymbol{x}\right)\phi_{0,g'}^0\left(\boldsymbol{x}\right)dV+\int_{V_j}w_j\left(\boldsymbol{x}\right)q_{n,g}\left(\boldsymbol{x}\right)dV,$$
$$j=1,\ldots,J,\quad n=1,\ldots N,\quad g=1,\ldots,G. \quad (22)$$

Perform integration by parts on the streaming term and apply the divergence theorem

$$\int_V\boldsymbol{\nabla}\cdot\boldsymbol{F}\left(\boldsymbol{x}\right)dV=\int_S\boldsymbol{n}\cdot\boldsymbol{F}\left(\boldsymbol{x}\right)dS \quad (23)$$

to get the weak form of the transport equation,

$$\int_{S_j}\left(\boldsymbol{\Omega}_n\cdot\boldsymbol{n}\right)\psi_{n,g}\left(\boldsymbol{x}\right)w_j\left(\boldsymbol{x}\right)dS-\int_{V_j}\psi_{n,g}\left(\boldsymbol{x}\right)\left[\boldsymbol{\Omega}\cdot\boldsymbol{\nabla}w_j\left(\boldsymbol{x}\right)\right]dV+\int_{V_j}w_j\left(\boldsymbol{x}\right)\Sigma_{t;g}\left(\boldsymbol{x}\right)\psi_{n,g}\left(\boldsymbol{x}\right)dV$$
$$=\sum_{\ell=0}^{\infty}\frac{2\ell+1}{4\pi}\sum_{m=-\ell}^{\ell}Y_\ell^m\left(\boldsymbol{\Omega}_n\right)\sum_{g'=1}^{G}\int_{V_j}w_j\left(\boldsymbol{x}\right)\Sigma_{s;\ell,g'\rightarrow g}\left(\boldsymbol{x}\right)\phi_{\ell,g'}^m\left(\boldsymbol{x}\right)dV$$
$$+\int_{V_j}w_j\left(\boldsymbol{x}\right)\frac{\chi_g\left(\boldsymbol{x}\right)}{4\pi}\sum_{g'=1}^{G}\nu\Sigma_{f;g'}\left(\boldsymbol{x}\right)\phi_{0,g'}^0\left(\boldsymbol{x}\right)dV+\int_{V_j}w_j\left(\boldsymbol{x}\right)q_{n,g}\left(\boldsymbol{x}\right)dV,$$

$$j = 1, \ldots, J, \quad n = 1, \ldots N, \quad g = 1, \ldots, G. \quad (24)$$

The surface integral can be split into its unknown and known parts (the boundary condition) to give

$$\begin{aligned}\int_{\boldsymbol{\Omega}_n \cdot \boldsymbol{n} > 0} (\boldsymbol{\Omega}_n \cdot \boldsymbol{n}) \, \psi_{n,g}(\boldsymbol{x}) \, w_j(\boldsymbol{x}) \, dS - \int_{V_j} \psi_{n,g}(\boldsymbol{x}) \left[\boldsymbol{\Omega} \cdot \boldsymbol{\nabla} w_j(\boldsymbol{x})\right] dV + \int_{V_j} w_j(\boldsymbol{x}) \, \Sigma_{t;g}(\boldsymbol{x}) \, \psi_{n,g}(\boldsymbol{x}) \, dV \\ = \sum_{\ell=0}^{\infty} \frac{2\ell+1}{4\pi} \sum_{m=-\ell}^{\ell} Y_\ell^m(\boldsymbol{\Omega}_n) \sum_{g'=1}^{G} \int_{V_j} w_j(\boldsymbol{x}) \, \Sigma_{s;\ell,g' \to g}(\boldsymbol{x}) \, \phi_{\ell,g'}^m(\boldsymbol{x}) \, dV \\ + \int_{V_j} w_j(\boldsymbol{x}) \frac{\chi_g(\boldsymbol{x})}{4\pi} \sum_{g'=1}^{G} \nu \Sigma_{f;g'}(\boldsymbol{x}) \, \phi_{0,g'}^0(\boldsymbol{x}) \, dV + \int_{\boldsymbol{\Omega}_n \cdot \boldsymbol{n} < 0} |\boldsymbol{\Omega}_n \cdot \boldsymbol{n}| \, \psi_{n,g}^b(\boldsymbol{x}) \, w_j(\boldsymbol{x}) \, dS \\ + \int_{V_j} w_j(\boldsymbol{x}) \, q_{n,g}(\boldsymbol{x}) \, dV \\ j = 1, \ldots, J, \quad n = 1, \ldots N, \quad g = 1, \ldots, G. \quad (25)\end{aligned}$$

If the cross sections are constant within each support region V_j, ($\Sigma_j = \Sigma(\boldsymbol{x})$ for all $\boldsymbol{x} \in V_j$) this simplifies to

$$\begin{aligned}\int_{\boldsymbol{\Omega}_n \cdot \boldsymbol{n} > 0} (\boldsymbol{\Omega}_n \cdot \boldsymbol{n}) \, \psi_{n,g}(\boldsymbol{x}) \, w_j(\boldsymbol{x}) \, dS - \int_{V_j} \psi_{n,g}(\boldsymbol{x}) \left[\boldsymbol{\Omega} \cdot \boldsymbol{\nabla} w_j(\boldsymbol{x})\right] dV + \Sigma_{t;j,g} \int_{V_j} w_j(\boldsymbol{x}) \, \psi_{n,g}(\boldsymbol{x}) \, dV \\ = \sum_{\ell=0}^{\infty} \frac{2\ell+1}{4\pi} \sum_{m=-\ell}^{\ell} Y_\ell^m(\boldsymbol{\Omega}_n) \sum_{g'=1}^{G} \Sigma_{s;j,\ell,g' \to g} \int_{V_j} w_j(\boldsymbol{x}) \, \phi_{\ell,g'}^m(\boldsymbol{x}) \, dV \\ + \frac{\chi_{j,g}}{4\pi} \sum_{g'=1}^{G} \nu \Sigma_{f;j,g'} \int_{V_j} w_j(\boldsymbol{x}) \, \phi_{0,g'}^0(\boldsymbol{x}) \, dV + \int_{\boldsymbol{\Omega}_n \cdot \boldsymbol{n} < 0} |\boldsymbol{\Omega}_n \cdot \boldsymbol{n}| \, \psi_{n,g}^b(\boldsymbol{x}) \, w_j(\boldsymbol{x}) \, dS \\ + \int_{V_j} w_j(\boldsymbol{x}) \, q_{n,g}(\boldsymbol{x}) \, dV, \\ j = 1, \ldots, J, \quad n = 1, \ldots N, \quad g = 1, \ldots, G. \quad (26)\end{aligned}$$

3.3 Conservation of neutrons

Without loss of generality, the weak form of the transport equation can be written as

$$\begin{aligned}\int_{\boldsymbol{\Omega}_n \cdot \boldsymbol{n} > 0} (\boldsymbol{\Omega}_n \cdot \boldsymbol{n}) \, \psi_{n,g}(\boldsymbol{x}) \, w_j(\boldsymbol{x}) \, dS - \int_{V_j} \psi_{n,g}(\boldsymbol{x}) \left[\boldsymbol{\Omega}_n \cdot \boldsymbol{\nabla} w_j(\boldsymbol{x})\right] dV + \int_{V_j} \Sigma_{t;g}(\boldsymbol{x}) \, w_j(\boldsymbol{x}) \, \psi_{n,g}(\boldsymbol{x}) \, dV \\ = \int_{V_j} w_j(\boldsymbol{x}) \, s_{n,g}(\boldsymbol{x}) \, dV + \int_{\boldsymbol{\Omega}_n \cdot \boldsymbol{n} < 0} |\boldsymbol{\Omega}_n \cdot \boldsymbol{n}| \, \psi_{n,g}^b(\boldsymbol{x}) \, w_j(\boldsymbol{x}) \, dS, \\ j = 1, \ldots, J, \quad n = 1, \ldots N, \quad g = 1, \ldots, G, \quad (27)\end{aligned}$$

where

$$\begin{aligned}s_{n,g}(\boldsymbol{x}) = \sum_{\ell=0}^{\infty} \frac{2\ell+1}{4\pi} \sum_{m=-\ell}^{\ell} Y_\ell^m(\boldsymbol{\Omega}_n) \sum_{g'=1}^{G} \Sigma_{s;\ell,g' \to g}(\boldsymbol{x}) \, \phi_{\ell,g'}^m(\boldsymbol{x}) \\ + \frac{\chi_g(\boldsymbol{x})}{4\pi} \sum_{g'=1}^{G} \nu \Sigma_{f;g'}(\boldsymbol{x}) \, \phi_{0,g'}^0(\boldsymbol{x}) + q_{n,g}(\boldsymbol{x}). \quad (28)\end{aligned}$$

Multiply the transport equation by an arbitrary constant c_j and sum over all j to get

$$\int_{\boldsymbol{\Omega}_n\cdot\boldsymbol{n}>0}\left(\boldsymbol{\Omega}_n\cdot\boldsymbol{n}\right)\psi_{n,g}\left(\boldsymbol{x}\right)\left(\sum_{j=1}^{J}c_j w_j\left(\boldsymbol{x}\right)\right)dS-\int_V \psi_{n,g}\left(\boldsymbol{x}\right)\left[\boldsymbol{\Omega}_n\cdot\boldsymbol{\nabla}\left(\sum_{j=1}^{J}c_j w_j\left(\boldsymbol{x}\right)\right)\right]dV$$
$$+\int_V \Sigma_{t;g}\left(\boldsymbol{x}\right)\left(\sum_{j=1}^{J}c_j w_j\left(\boldsymbol{x}\right)\right)\psi_{n,g}\left(\boldsymbol{x}\right)dV$$
$$=\int_V\left(\sum_{j=1}^{J}c_j w_j\left(\boldsymbol{x}\right)\right)s_{n,g}\left(\boldsymbol{x}\right)dV+\int_{\boldsymbol{\Omega}_n\cdot\boldsymbol{n}<0}\left|\boldsymbol{\Omega}_n\cdot\boldsymbol{n}\right|\psi^b_{n,g}\left(\boldsymbol{x}\right)\left(\sum_{j=1}^{J}c_j w_j\left(\boldsymbol{x}\right)\right)dS,$$
$$n=1,\ldots N,\quad g=1,\ldots,G. \tag{29}$$

Suppose that there exist c_j such that

$$\sum_j c_j w_j\left(\boldsymbol{x}\right)=1. \tag{30}$$

Then using these c_j, we get that the weak form of the transport equations satisfy

$$\int_{\boldsymbol{\Omega}_n\cdot\boldsymbol{n}>0}\left(\boldsymbol{\Omega}_n\cdot\boldsymbol{n}\right)\psi_{n,g}\left(\boldsymbol{x}\right)dS-\int_{\boldsymbol{\Omega}_n\cdot\boldsymbol{n}<0}\left|\boldsymbol{\Omega}_n\cdot\boldsymbol{n}\right|\psi^b_{n,g}\left(\boldsymbol{x}\right)dS=\int_V s_{n,g}\left(\boldsymbol{x}\right)dV-\int_V\Sigma_{t,g}\left(\boldsymbol{x}\right)\psi_{n,g}\left(\boldsymbol{x}\right)dV,$$
$$n=1,\ldots N,\quad g=1,\ldots,G. \tag{31}$$

This statement of conservation can also be directly derived by integrating the transport equation over V. It states that the neutrons entering the problem minus the neutrons exiting the problem equal the gains from the internal source, scattering and fission plus the losses from absorption. Thus, it is a sufficient condition for conservation that Eq. 30 holds true for some c_j.

3.4 Petrov-Galerkin method

The Petrov-Galerkin method can supply the unknowns needed to solve the weak form of the transport equation. Defining

$$\psi_{n,g}\left(\boldsymbol{x}\right)=\sum_{i=1}^{J}\alpha_{i,n,g}b_i\left(\boldsymbol{x}\right), \tag{32a}$$
$$\phi^m_{\ell,g}\left(\boldsymbol{x}\right)=\sum_{n=1}^{N}Y^m_\ell\left(\boldsymbol{\Omega}_n\right)\sum_{i=1}^{J}\alpha_{i,n,g}b_i\left(\boldsymbol{x}\right)=\sum_{i=1}^{J}\beta^m_{i,\ell,g}b_i\left(\boldsymbol{x}\right), \tag{32b}$$
$$\psi^b_{n,g}\left(\boldsymbol{x}\right)=\sum_{i=1}^{J}\alpha^b_{i,n,g}b_i\left(\boldsymbol{x}\right), \tag{32c}$$

as the basis, the weak form of the transport equation becomes

$$\sum_{i=1}^{J}\left[\int_{\boldsymbol{\Omega}_n\cdot\boldsymbol{n}>0}\left(\boldsymbol{\Omega}_n\cdot\boldsymbol{n}\right)b_i\left(\boldsymbol{x}\right)w_j\left(\boldsymbol{x}\right)dS-\int_{V_j}b_i\left(\boldsymbol{x}\right)\left[\boldsymbol{\Omega}_n\cdot\boldsymbol{\nabla}w_j\left(\boldsymbol{x}\right)\right]dV+\Sigma_{t;j,g}\int_{V_j}b_i\left(\boldsymbol{x}\right)w_j\left(\boldsymbol{x}\right)dV\right]\alpha_{i,n,g}$$
$$=\sum_\ell\frac{2\ell+1}{4\pi}\sum_m Y^m_\ell\left(\boldsymbol{\Omega}_n\right)\sum_{g'}\Sigma_{s;j,\ell,g'\to g}\sum_{i=1}^{J}\beta^m_{i,\ell,g'}\int_{V_j}b_i\left(\boldsymbol{x}\right)w_j\left(\boldsymbol{x}\right)dV$$
$$+\frac{\chi_{j,g}}{4\pi}\sum_{g'}\nu\Sigma_{f;j,g'}\sum_{i=1}^{J}\beta^0_{i,0,g'}\int_{V_j}b_i\left(\boldsymbol{x}\right)w_j\left(\boldsymbol{x}\right)dV+\sum_{i=1}^{J}\alpha^b_{i,n,g}\int_{\boldsymbol{\Omega}_n\cdot\boldsymbol{n}<0}\left|\boldsymbol{\Omega}_n\cdot\boldsymbol{n}\right|b_i\left(\boldsymbol{x}\right)w_j\left(\boldsymbol{x}\right)dS$$
$$+\int_{V_j}w_j\left(\boldsymbol{x}\right)q_{n,g}\left(\boldsymbol{x}\right)dV,$$
$$j=1,\ldots,J,\quad n=1,\ldots N,\quad g=1,\ldots,G. \tag{33}$$

Thus, the integrands become functions of the known b_i, w_j, and $q_{n,g}$. If $b_i = w_i$ for all i, this is the Galerkin method, which is frequently used in the finite element method. If the basis and weight function differ, it is the Petrov-Galerkin method. Note that the relationship between the $\alpha_{i,n,g}$ and $\beta^m_{i,\ell,g}$ is exactly the same as $\psi_{n,g}$ and $\phi^m_{\ell,g}$:

$$\beta^m_{i,\ell,g} = \sum_{n=1}^{N} w_n Y^m_\ell \left(\boldsymbol{\Omega}_n\right) \alpha_{i,n,g}. \tag{34}$$

This allows the same code that is used to convert between the angular flux and its moments to do the same for α and β. The boundary source term is written in a form that allows easy reflection without interpolation. If instead of reflection the boundary source is intrinsic to the problem, the boundary source itself could be used in the integrand.

3.5 Streamline upwind Petrov-Galerkin method

The streamline upwind Petrov-Galerkin (SUPG) method can be used to stabilize the solution of the transport equation when a continuous method (such as the CFEM, or continuous finite element method) is used. In these methods, the solution does not allow discontinuities. Because the transport equation is mathematically an advection equation, this causes instabilities that manifest in oscillations. The SUPG method adds artificial diffusion into the problem without affecting overall particle balance. Using the definition of $s_{n,g}$ in Eq. 28, the weak form of the transport equation before integration by parts is

$$\begin{aligned}\int_{V_j} w_j\left(\boldsymbol{x}\right)\left[\boldsymbol{\Omega}_n \cdot \boldsymbol{\nabla}\psi_{n,g}\left(\boldsymbol{x}\right)\right] dV + \int_{V_j} \Sigma_{t;g}\left(\boldsymbol{x}\right) w_j\left(\boldsymbol{x}\right)\psi_{n,g}\left(\boldsymbol{x}\right) dV \\ = \int_{V_j} w_j\left(\boldsymbol{x}\right) s_{n,g}\left(\boldsymbol{x}\right) dV, \\ j = 1,\ldots,J, \quad n = 1,\ldots N, \quad g = 1,\ldots,G,\end{aligned} \tag{35}$$

If instead of using the weight function $w_j\left(\boldsymbol{x}\right)$ we used as a weight function $\boldsymbol{\Omega}_n \cdot \boldsymbol{\nabla} w_j\left(\boldsymbol{x}\right)$, this equation would become

$$\begin{aligned}\int_{V_j} \left[\boldsymbol{\Omega}_n \cdot \boldsymbol{\nabla} w_j\left(\boldsymbol{x}\right)\right]\left[\boldsymbol{\Omega}_n \cdot \boldsymbol{\nabla}\psi_{n,g}\left(\boldsymbol{x}\right)\right] dV + \int_{V_j} \Sigma_{t;g}\left(\boldsymbol{x}\right)\left[\boldsymbol{\Omega}_n \cdot \boldsymbol{\nabla} w_j\left(\boldsymbol{x}\right)\right]\psi_{n,g}\left(\boldsymbol{x}\right) dV \\ = \int_{V_j} \left[\boldsymbol{\Omega}_n \cdot \boldsymbol{\nabla} w_j\left(\boldsymbol{x}\right)\right] s_{n,g}\left(\boldsymbol{x}\right) dV, \\ j = 1,\ldots,J, \quad n = 1,\ldots N, \quad g = 1,\ldots,G,\end{aligned} \tag{36}$$

Adding this equation to Eq. 27 gives the SUPG form of the transport equation,

$$\begin{aligned}\int_{\boldsymbol{\Omega}_n\cdot\boldsymbol{n}>0} \left(\boldsymbol{\Omega}_n \cdot \boldsymbol{n}\right)\psi_{n,g}\left(\boldsymbol{x}\right) w_j\left(\boldsymbol{x}\right) dS + \int_{V_j}\left[\psi_{n,g}\left(\boldsymbol{x}\right) + \boldsymbol{\Omega}_n \cdot \boldsymbol{\nabla}\psi_{n,g}\left(\boldsymbol{x}\right)\right]\left[\boldsymbol{\Omega}_n \cdot \boldsymbol{\nabla} w_j\left(\boldsymbol{x}\right)\right] dV \\ + \int_{V_j} \Sigma_{t;g}\left(\boldsymbol{x}\right)\left[w_j\left(\boldsymbol{x}\right) + \boldsymbol{\Omega}_n \cdot \boldsymbol{\nabla} w_j\left(\boldsymbol{x}\right)\right]\psi_{n,g}\left(\boldsymbol{x}\right) dV \\ = \int_{V_j}\left[w_j\left(\boldsymbol{x}\right) + \boldsymbol{\Omega}_n \cdot \boldsymbol{\nabla} w_j\left(\boldsymbol{x}\right)\right] s_{n,g}\left(\boldsymbol{x}\right) dV + \int_{\boldsymbol{\Omega}_n\cdot\boldsymbol{n}<0} \left|\boldsymbol{\Omega}_n \cdot \boldsymbol{n}\right| \psi^b_{n,g}\left(\boldsymbol{x}\right) w_j\left(\boldsymbol{x}\right) dS, \\ j = 1,\ldots,J, \quad n = 1,\ldots N, \quad g = 1,\ldots,G,\end{aligned} \tag{37}$$

Notably, this addition does not affect particle balance if Eq. 30 holds as before, as the derivatives will annihilate the constant, giving $0 = 0$ for the SUPG addition when multiplied by c_j and summed over all j. The reason this term stabilizes the method can be found in the volume integral of the streaming term. If we had a diffusion method with diffusion tensor $\boldsymbol{D} = \boldsymbol{\Omega}_n\boldsymbol{\Omega}_n$,

$$-\left(\boldsymbol{\Omega}_n \cdot \boldsymbol{\nabla}\right)\left(\boldsymbol{\Omega}_n \cdot \boldsymbol{\nabla}\right) f\left(\boldsymbol{x}\right) = -\boldsymbol{\nabla} \cdot \left(\boldsymbol{D} \cdot \boldsymbol{\nabla}\right) f\left(\boldsymbol{x}\right) = 0, \tag{38}$$

the weak form of the equation would be

$$-\int_{S_j}\left[\boldsymbol{n}\cdot\left(\boldsymbol{D}\cdot\boldsymbol{\nabla}\right)f\left(\boldsymbol{x}\right)\right]w_j\left(\boldsymbol{x}\right)+\int_{V_j}\left[\boldsymbol{\Omega}_n\cdot\boldsymbol{\nabla}f\left(\boldsymbol{x}\right)\right]\left[\boldsymbol{\Omega}_n\cdot\boldsymbol{\nabla}w_j\left(\boldsymbol{x}\right)\right]dV=0. \tag{39}$$

The diffusive term in Eq. 39 can be found in the SUPG addition in Eq. 37. This adds numerical diffusion (and stabilization) to the method.

3.6 Spatially-dependent cross sections

THINK ABOUT HOW TO HANDLE SPHERICAL HARMONIC MOMENTS OF Σ_s: DEPENDS ON m

Suppose that the assumption made after Eq. 25 that the cross sections are continuous does not hold. The integrals over weight and basis functions would then have to be done for each group and cross section as well. To avoid this, some approximation of the moments of the angular flux $\Phi^m_{\ell,g}\left(\boldsymbol{x}\right)$ (from a low-order P_N or SP_N calculation, for instance) can be used to weight the cross sections and remove them from the integrals. Define

$$\Sigma_{t;j,g}\equiv\frac{\int_{V_j}\Sigma_{t;g}\left(\boldsymbol{x}\right)\Phi^0_{0,g}\left(\boldsymbol{x}\right)w_j\left(\boldsymbol{x}\right)dV}{\int_{V_j}\Phi^0_{0,g}\left(\boldsymbol{x}\right)w_j\left(\boldsymbol{x}\right)dV}, \tag{40a}$$

$$\Sigma_{s;j,\ell,g'\rightarrow g}\equiv\frac{\int_{V_j}\Sigma_{s;\ell,g'\rightarrow g}\left(\boldsymbol{x}\right)\Phi^m_{\ell,g'}\left(\boldsymbol{x}\right)w_j\left(\boldsymbol{x}\right)dV}{\int_{V_j}\Phi^m_{\ell,g'}\left(\boldsymbol{x}\right)w_j\left(\boldsymbol{x}\right)dV}, \tag{40b}$$

$$\chi_{j,g}\equiv\frac{\int_{V_j}\chi_g\left(\boldsymbol{x}\right)\sum_{g'}\left[\nu\Sigma_{f;g'}\Phi^0_{0,g'}\left(\boldsymbol{x}\right)\right]w_j\left(\boldsymbol{x}\right)dV}{\int_{V_j}\sum_{g'}\left[\nu\Sigma_{f;g'}\Phi^0_{0,g'}\left(\boldsymbol{x}\right)\right]w_j\left(\boldsymbol{x}\right)dV}, \tag{40c}$$

$$\nu\Sigma_{f;j,g}\equiv\frac{\int_{V_j}\nu\Sigma_{f;g}\left(\boldsymbol{x}\right)\Phi^0_{0,g}\left(\boldsymbol{x}\right)w_j\left(\boldsymbol{x}\right)dV}{\int_{V_j}\Phi^0_{0,g}\left(\boldsymbol{x}\right)w_j\left(\boldsymbol{x}\right)dV}, \tag{40d}$$

(noting that the fission spectrum is weighted by the fission source) and assume that

$$\phi^0_{0,g}\left(\boldsymbol{x}\right)\sim\psi_{n,g}\left(\boldsymbol{x}\right)\ \text{ for all } n,g, \tag{41a}$$

$$\Phi^m_{\ell,g}\sim\phi^m_{\ell,g}\ \text{ for all } \ell,m,g. \tag{41b}$$

Then the approximations can be made that

$$\begin{aligned}\int_{V_j}w_j\left(\boldsymbol{x}\right)\Sigma_{t,g}\left(\boldsymbol{x}\right)\psi_{n,g}\left(\boldsymbol{x}\right)dV&\\ \approx\frac{\int_{V_j}\Sigma_{t;g}\left(\boldsymbol{x}\right)\Phi^0_{0,g}\left(\boldsymbol{x}\right)w_j\left(\boldsymbol{x}\right)dV}{\int_{V_j}\Phi^0_{0,g}\left(\boldsymbol{x}\right)w_j\left(\boldsymbol{x}\right)dV}&\int_{V_j}w_j\left(\boldsymbol{x}\right)\psi_{n,g}\left(\boldsymbol{x}\right)dV\\ =\Sigma_{t;j,g}&\int_{V_j}w_j\left(\boldsymbol{x}\right)\psi_{n,g}\left(\boldsymbol{x}\right)dV,\end{aligned} \tag{42a}$$

$$\begin{aligned}\int_{V_j}w_j\left(\boldsymbol{x}\right)\Sigma_{s;\ell,g'\rightarrow g}\left(\boldsymbol{x}\right)\phi^m_{\ell,g'}\left(\boldsymbol{x}\right)dV&\\ \approx\frac{\int_{V_j}\Sigma_{s;\ell,g'\rightarrow g}\left(\boldsymbol{x}\right)\Phi^m_{\ell,g'}\left(\boldsymbol{x}\right)w_j\left(\boldsymbol{x}\right)dV}{\int_{V_j}\Phi^m_{\ell,g'}\left(\boldsymbol{x}\right)w_j\left(\boldsymbol{x}\right)dV}&\int_{V_j}w_j\left(\boldsymbol{x}\right)\phi^m_{\ell,g'}\left(\boldsymbol{x}\right)dV\\ =\Sigma_{s;j,\ell,g'\rightarrow g}&\int_{V_j}w_j\left(\boldsymbol{x}\right)\phi^m_{\ell,g'}\left(\boldsymbol{x}\right)dV,\end{aligned} \tag{42b}$$

$$\int_{V_j} w_j(\boldsymbol{x})\,\chi_g(\boldsymbol{x}) \sum_{g'=1}^{G} \nu\Sigma_{f;g'}(\boldsymbol{x})\,\phi^0_{0,g'}(\boldsymbol{x})\,dV$$

$$\approx \frac{\int_{V_j} \chi_g(\boldsymbol{x}) \sum_{g''} \left[\nu\Sigma_{f;g''}\Phi^0_{0,g''}(\boldsymbol{x})\right] w_j(\boldsymbol{x})\,dV}{\int_{V_j} \sum_{g''} \left[\nu\Sigma_{f;g''}\Phi^0_{0,g''}(\boldsymbol{x})\right] w_j(\boldsymbol{x})\,dV} \sum_{g'=1}^{G} \frac{\int_{V_j} \nu\Sigma_{f;g'}(\boldsymbol{x})\,\Phi^0_{0,g'}(\boldsymbol{x})\,w_j(\boldsymbol{x})\,dV}{\int_{V_j} \Phi^0_{0,g'}(\boldsymbol{x})\,w_j(\boldsymbol{x})\,dV} \int_{V_j} \phi^0_{0,g'}(\boldsymbol{x})\,w_j(\boldsymbol{x})\,dV$$

$$= \chi_{g,j} \sum_{g'=1}^{G} \nu\Sigma_{f;j,g'} \int_{V_j} \phi^0_{0,g'}(\boldsymbol{x})\,w_j(\boldsymbol{x})\,dV. \quad (42c)$$

If instead of using only the first spherical harmonic moment of the angular flux in Eq. 40a a more complete weighting using the spherical harmonic expansion (Eq. 6) were used, the approximation would be instead

$$\Sigma_{t;j,g,n} \equiv \frac{\sum_{\ell=0}^{\infty} \frac{2\ell+1}{4\pi} \sum_{m=-\ell}^{\ell} Y_\ell^m(\boldsymbol{\Omega}_n) \int_{V_j} \Sigma_{t;g}(\boldsymbol{x})\,\Phi^m_{\ell,g}(\boldsymbol{x})\,w_j(\boldsymbol{x})\,dV}{\sum_{\ell=0}^{\infty} \frac{2\ell+1}{4\pi} \sum_{m=-\ell}^{\ell} Y_\ell^m(\boldsymbol{\Omega}_n) \int_{V_j} \Phi^m_{\ell,g}(\boldsymbol{x})\,w_j(\boldsymbol{x})\,dV}. \quad (43)$$

This approximation would be truncated to some finite value of ℓ. The values for each n could be calculated as needed and would not need to be stored. This would increase the number of integrals, but not significantly when compared, for instance, to the number required for the scattering cross section.

Part II
Spatial approximations to the transport equation

4 Derivation of the diffusion equations

4.1 From spatially continuous transport equations

In this derivation, ϕ_g will be the multigroup isotropic moment of the angular flux, while $\boldsymbol{J}$ will be the multigroup current. These are defined in terms of the spherical harmonic moments as as

$$\phi_g \equiv \phi_{0,g}^0, \tag{44a}$$

$$\boldsymbol{J}_g \equiv \left[\phi_{1,g}^0, \phi_{1,g}^1, \phi_{1,g}^{-1}\right]. \tag{44b}$$

The linearly anisotropic (or first-order) flux approximation can then be written

$$\begin{aligned}\psi_g(\boldsymbol{x}, \boldsymbol{\Omega}, t) &\approx \sum_{\ell=0}^{1} \frac{2\ell+1}{4\pi} \sum_{m=-\ell}^{\ell} \phi_\ell^m(\boldsymbol{x}, t) Y_\ell^m(\boldsymbol{\Omega})\, d\Omega \\ &= \frac{1}{4\pi}\left[\phi_g(\boldsymbol{x}, t) + 3\boldsymbol{\Omega}\cdot\boldsymbol{J}_g(\boldsymbol{x}, t)\right].\end{aligned} \tag{45}$$

We also define the zeroth and first order sources as

$$Q_{0,g}(\boldsymbol{x}, t) \equiv \frac{1}{4\pi}\int_{4\pi} q_g(\boldsymbol{x}, \boldsymbol{\Omega}, t)\, d\Omega,$$

$$\boldsymbol{Q}_{1,g}(\boldsymbol{x}, t) \equiv \frac{1}{4\pi}\int_{4\pi} \boldsymbol{\Omega} q_g(\boldsymbol{x}, \boldsymbol{\Omega}, t)\, d\Omega.$$

Beginning from the multigroup, continuous-energy and space equation (Eq. 12) with its accompanying boundary and initial conditions (Eq. 13), perform $\int_{4\pi}(\cdot)\, d\Omega$ and $\int_{4\pi}\boldsymbol{\Omega}(\cdot)\, d\Omega$ individually to get

$$\begin{aligned}&\frac{1}{v_g(\boldsymbol{x})}\frac{\partial}{\partial t}\phi_g(\boldsymbol{x}) + \boldsymbol{\nabla}\cdot\boldsymbol{J}_g(\boldsymbol{x}, t) + \Sigma_{t;g}(\boldsymbol{x})\phi_g(\boldsymbol{x}) \\ &\qquad = \sum_{g'=1}^{G}\Sigma_{s;0,g'\to g}(\boldsymbol{x})\phi_{g'}(\boldsymbol{x}, t) + \frac{\chi_g(\boldsymbol{x})}{4\pi}\sum_{g'=1}^{G}\nu\Sigma_{f;g'}(\boldsymbol{x})\phi_{g'}(\boldsymbol{x}, t) + Q_{0,g}(\boldsymbol{x}, t), \\ &\qquad\qquad \boldsymbol{x}\in V, \quad g = 1, \ldots, G, \quad 0 < t,\end{aligned} \tag{47a}$$

$$\begin{aligned}&\frac{1}{v_g(\boldsymbol{x})}\frac{\partial}{\partial t}\boldsymbol{J}_g(\boldsymbol{x}) + \frac{1}{3}\boldsymbol{\nabla}\phi_g(\boldsymbol{x}, t) + \Sigma_{t;g}(\boldsymbol{x})\boldsymbol{J}_g(\boldsymbol{x}) \\ &\qquad = \sum_{g'=1}^{G}\Sigma_{s;1,g'\to g}(\boldsymbol{x})\boldsymbol{J}_{g'}(\boldsymbol{x}, t), \\ &\qquad\qquad \boldsymbol{x}\in V, \quad g = 1, \ldots, G, \quad 0 < t.\end{aligned} \tag{47b}$$

Neglect time derivative on $\boldsymbol{J}$ and assume that

$$\sum_{g'=1}^{G}\Sigma_{s;1,g'\to g}(\boldsymbol{x})\boldsymbol{J}_{g'}(\boldsymbol{x}, t) \approx \boldsymbol{J}_g(\boldsymbol{x}, t)\sum_{g'=1}^{G}\Sigma_{s;1,g'\to g} \tag{48}$$

(i.e. the energy and direction of scattering are independent) to get Fick's Law,

$$\boldsymbol{J}_g(\boldsymbol{x}, t) \approx -D_g(\boldsymbol{x})\boldsymbol{\nabla}\phi_g(\boldsymbol{x}, t), \tag{49}$$

with

$$\Sigma_{tr;g}(\boldsymbol{x}) \equiv \Sigma_{t;g}(\boldsymbol{x}) - \sum_{g'=1}^{G} \Sigma_{s;1,g'\to g}, \tag{50a}$$

$$D_g(\boldsymbol{x}) \equiv \frac{1}{3\Sigma_{tr;g}(\boldsymbol{x})}. \tag{50b}$$

Then the multigroup diffusion equation is

$$\frac{1}{v_g(\boldsymbol{x})}\frac{\partial}{\partial t}\phi_g(\boldsymbol{x},t) - \boldsymbol{\nabla}\cdot D_g(\boldsymbol{x})\boldsymbol{\nabla}\phi_g(\boldsymbol{x},t) + \Sigma_{t;g}(\boldsymbol{x})\phi_g(\boldsymbol{x},t)$$
$$= \sum_{g'=1}^{G} \Sigma_{s;0,g'\to g}(\boldsymbol{x})\phi_{g'}(\boldsymbol{x},t) + \frac{\chi_g(\boldsymbol{x})}{4\pi}\sum_{g'=1}^{G}\nu\Sigma_{f;g'}(\boldsymbol{x})\phi_{g'}(\boldsymbol{x},t) + Q_{0,g}(\boldsymbol{x},t),$$
$$\boldsymbol{x}\in V, \quad g=1,\ldots,G, \quad 0<t. \tag{51}$$

For the boundary condition, start by defining incoming and outgoing partial currents,

$$J_g^-(\boldsymbol{x},t) \equiv \int_{\boldsymbol{\Omega}\cdot\boldsymbol{n}<0} |\boldsymbol{\Omega}\cdot\boldsymbol{n}|\,\psi_g(\boldsymbol{x},\boldsymbol{\Omega},t)\,d\Omega, \tag{52a}$$

$$J_g^+(\boldsymbol{x},t) \equiv \int_{\boldsymbol{\Omega}\cdot\boldsymbol{n}>0} \boldsymbol{\Omega}\cdot\boldsymbol{n}\psi_g(\boldsymbol{x},\boldsymbol{\Omega},t)\,d\Omega, \tag{52b}$$

, and using the linearly anisotropic assumption to get

$$J_g^-(\boldsymbol{x},t) \approx -\frac{1}{4\pi}\boldsymbol{n}\cdot\left[\int_{\boldsymbol{\Omega}\cdot\boldsymbol{n}<0}\boldsymbol{\Omega}\phi_g(\boldsymbol{x},t) + 3\boldsymbol{\Omega}\boldsymbol{\Omega}\cdot\boldsymbol{J}_g(\boldsymbol{x},t)\,d\Omega\right] = \frac{1}{4}\left[\phi_g(\boldsymbol{x},t) - 2\boldsymbol{n}\cdot\boldsymbol{J}_g(\boldsymbol{x},t)\right], \tag{53a}$$

$$J_g^+(\boldsymbol{x},t) \approx \frac{1}{4\pi}\boldsymbol{n}\cdot\left[\int_{\boldsymbol{\Omega}\cdot\boldsymbol{n}>0}\boldsymbol{\Omega}\phi_g(\boldsymbol{x},t) + 3\boldsymbol{\Omega}\boldsymbol{\Omega}\cdot\boldsymbol{J}_g(\boldsymbol{x},t)\,d\Omega\right] = \frac{1}{4}\left[\phi_g(\boldsymbol{x},t) + 2\boldsymbol{n}\cdot\boldsymbol{J}_g(\boldsymbol{x},t)\right]. \tag{53b}$$

Apply Fick's Law to get these in terms of the scalar flux,

$$J_g^-(\boldsymbol{x},t) = \frac{1}{4}\left[\phi_g(\boldsymbol{x},t) + 2D_g(\boldsymbol{x})\boldsymbol{n}\cdot\boldsymbol{\nabla}\phi_g(\boldsymbol{x},t)\right], \tag{54a}$$

$$J_g^+(\boldsymbol{x},t) = \frac{1}{4}\left[\phi_g(\boldsymbol{x},t) - 2D_g(\boldsymbol{x})\boldsymbol{n}\cdot\boldsymbol{\nabla}\phi_g(\boldsymbol{x},t)\right]. \tag{54b}$$

Multiply Eq. 13a by $|\boldsymbol{\Omega}\cdot\boldsymbol{n}|$ and integrate over those directions with $\boldsymbol{\Omega}\cdot\boldsymbol{n}<0$ to get

$$J_g^-(\boldsymbol{x},t) = J_g^{b-}(\boldsymbol{x},t) + \rho J_g^+(\boldsymbol{x},t). \tag{55}$$

This can be simplified further by using the definition of $\boldsymbol{J}$ in Eq. 49 to get the diffusion boundary condition,

$$\frac{1}{4}\left[(1-\rho)\phi_g(\boldsymbol{x},t) + 2(1+\rho)D_g(\boldsymbol{x})\boldsymbol{n}\cdot\boldsymbol{\nabla}\phi_g(\boldsymbol{x},t)\right] = J_g^{b-}(\boldsymbol{x},t). \tag{56a}$$

The initial condition can be found by performing $\int_{4\pi}(\cdot)\,d\Omega$ on the initial condition (Eq. 13b) to get

$$\phi_g(\boldsymbol{x},0) = \int_{4\pi}\psi_g^i(\boldsymbol{x},t)\,d\Omega \equiv \phi_g^i(\boldsymbol{x},t). \tag{56b}$$

4.1.1 Steady-state

For the steady-state diffusion equation, set the time derivative in Eq. 51 to zero and remove time dependence in the unknowns to get

$$-\boldsymbol{\nabla}\cdot D_g(\boldsymbol{x})\boldsymbol{\nabla}\phi_g(\boldsymbol{x}) + \Sigma_{t;g}(\boldsymbol{x})\phi_g(\boldsymbol{x})$$
$$= \sum_{g'=1}^{G}\Sigma_{s;0,g'\to g}(\boldsymbol{x})\phi_{g'}(\boldsymbol{x}) + \frac{\chi_g(\boldsymbol{x})}{4\pi}\sum_{g'=1}^{G}\nu\Sigma_{f;g'}(\boldsymbol{x})\phi_{g'}(\boldsymbol{x}) + Q_{0,g}(\boldsymbol{x}),$$
$$\boldsymbol{x}\in V, \quad g=1,\ldots,G. \tag{57}$$

4.2 From spatially discretized transport equations

Another possible method to derive the diffusion equations is to start at the spatially and angularly-discretized transport equation and calculate a discrete approximation to the transport discretization. Although untested, this could possibly allow use of DSA in problems that would otherwise lack consistency between the transport and diffusion discretizations.

- Define ϕ and $\boldsymbol{J}$ in a discrete way as the sums of weights
- Define coefficents β and γ as the expansion coefficients for ϕ and $\boldsymbol{J}$
- Perform $\sum_n w_n(\cdot)$ and $\sum_n w_n \boldsymbol{\Omega}_n(\cdot)$ over discretized equation (Eq. 21 or 33)
- Define matrices for each part of the equation
- Solve the second equation for $\boldsymbol{J}_g$
- Insert this solution (which will involve a matrix inverse) into the first equation

5 Spatial discretization of the diffusion equations

5.1 Strong discretization

The derivation of the strong form of the diffusion equations is identical to the derivation for the angular flux. Use the expansion in Eq. 32b in the diffusion equation and evaluate at discrete centers $\boldsymbol{x}_i$ to get

$$\sum_{i=1}^{J}\left[-D_g(\boldsymbol{x}_j)\nabla^2 b_i(\boldsymbol{x}_j)+\Sigma_{t;g}(\boldsymbol{x})\,b_i(\boldsymbol{x}_j)\right]\beta_{i,g} = \sum_{g'=1}^{G}\Sigma_{s;0,g'\to g}(\boldsymbol{x}_j)\,\phi_{g'}(\boldsymbol{x}_j)+\frac{\chi_g(\boldsymbol{x}_j)}{4\pi}\sum_{g'=1}^{G}\nu\Sigma_{f;g'}(\boldsymbol{x}_j)\,\phi_{g'}(\boldsymbol{x}_j)+Q_{0,g}(\boldsymbol{x}_j), \quad j=1,\ldots,J, \quad g=1,\ldots,G. \tag{58}$$

The ϕ values on the RHS can also be expressed in terms of $\beta_{i,g}$ if desired, or the system can be written in terms of $\phi_{i,g}$ with some localization procedure. The boundary conditions are

$$\frac{1}{4}\sum_{i=1}^{J}\left[(1-\rho)\,b_i(\boldsymbol{x})+2(1+\rho)\,D_g(\boldsymbol{x})\,\boldsymbol{n}\cdot\boldsymbol{\nabla}b_i(\boldsymbol{x})\right]\beta_{i,g}=J_g^{b-}(\boldsymbol{x}), \qquad j=1,\ldots,J, \quad g=1,\ldots,G.$$

5.2 Weak discretization

To derive the weak form of the diffusion equations, we take a few steps back to Eq. 47a to correctly account for the incoming and outgoing partial currents. Neglect the time derivative, assume the cross sections are constant or weighted in each integration region and apply $\int_{V_j} w_j(\cdot)\,dV$ to get

$$\int_{V_j} w_j(\boldsymbol{x})\,\boldsymbol{\nabla}\cdot\boldsymbol{J}_g(\boldsymbol{x})\,dV+\Sigma_{t;j,g}\int_{V_j} w_j(\boldsymbol{x})\,\phi_g(\boldsymbol{x})\,dV = \sum_{g'=1}^{G}\Sigma_{s;j,0,g'\to g}\int_{V_j} w_j(\boldsymbol{x})\,\phi_{g'}(\boldsymbol{x})\,dV+\frac{\chi_{j,g}}{4\pi}\sum_{g'=1}^{G}\nu\Sigma_{f;j,g'}\int_{V_j} w_j(\boldsymbol{x})\,\phi_{g'}(\boldsymbol{x})\,dV + \int_{V_j} w_j(\boldsymbol{x})\,Q_{0,g}(\boldsymbol{x})\,dV,$$

$$\boldsymbol{x} \in V, \quad g = 1, \ldots, G, \quad 0 < t. \tag{59}$$

Use the definitions of J^+ and J^- to derive a relationship with $\boldsymbol{J}$,

$$\begin{aligned}
\boldsymbol{n} \cdot \boldsymbol{J}_g(\boldsymbol{x}) &= \boldsymbol{n} \cdot \int_{4\pi} \boldsymbol{\Omega} \psi_g(\boldsymbol{x}, \boldsymbol{\Omega}) \, d\Omega \\
&= \int_{\boldsymbol{\Omega}\cdot\boldsymbol{n}>0} \boldsymbol{\Omega} \cdot \boldsymbol{n} \psi_g(\boldsymbol{x}, \boldsymbol{\Omega}) \, d\Omega - \int_{\boldsymbol{\Omega}\cdot\boldsymbol{n}<0} \boldsymbol{\Omega} \cdot \boldsymbol{n} \psi_g(\boldsymbol{x}, \boldsymbol{\Omega}) \, d\Omega \\
&= J_g^+(\boldsymbol{x}) - J_g^-(\boldsymbol{x}).
\end{aligned}$$

The streaming term then becomes

$$\int_{V_j} w_j(\boldsymbol{x}) \, \boldsymbol{\nabla} \cdot \boldsymbol{J}_g(\boldsymbol{x}) \, dV = \int_{S_j} w_j(\boldsymbol{x}) \left(\boldsymbol{n} \cdot \boldsymbol{J}(\boldsymbol{x})\right) dS - \int_{V_j} \left[\boldsymbol{\nabla} w_j(\boldsymbol{x})\right] \cdot \boldsymbol{J}(\boldsymbol{x}) \, dV \tag{60}$$

$$= \int_{S_j} w_j(\boldsymbol{x}) \left[J_g^+(\boldsymbol{x}) - J_g^-(\boldsymbol{x})\right] dS - \int_{V_j} \left[\boldsymbol{\nabla} w_j(\boldsymbol{x})\right] \cdot \boldsymbol{J}(\boldsymbol{x}) \, dV. \tag{61}$$

To review, J_g^+ represents the outgoing flux at the boundary (which we do not know a priori) and J_g^- represents the incoming flux at the boundary (which is known for the boundary source but not for reflection). Using Eq. 55, this the streaming term can be expanded to include the boundary condition,

$$\int_{S_j} w_j(\boldsymbol{x}) \left[J_g^+(\boldsymbol{x}) - J_g^-(\boldsymbol{x})\right] dS = \int_{S_j} w_j(\boldsymbol{x}) \left[(1-\rho) J_g^+(\boldsymbol{x}) - J_g^{b-}(\boldsymbol{x})\right] dS.$$

Putting the transport equation back together, we get

$$\begin{aligned}
(1-\rho) \int_{S_j} w_j(\boldsymbol{x}) \, J_g^+(\boldsymbol{x}) \, dS &- \int_{V_j} \left[\boldsymbol{\nabla} w_j(\boldsymbol{x})\right] \cdot \boldsymbol{J}(\boldsymbol{x}) \, dV + \Sigma_{t;j,g} \int_{V_j} w_j(\boldsymbol{x}) \, \phi_g(\boldsymbol{x}) \, dV \\
&= \sum_{g'=1}^{G} \Sigma_{s;j,0,g'\to g} \int_{V_j} w_j(\boldsymbol{x}) \, \phi_{g'}(\boldsymbol{x}) \, dV + \frac{\chi_{j,g}}{4\pi} \sum_{g'=1}^{G} \nu\Sigma_{f;j,g'} \int_{V_j} w_j(\boldsymbol{x}) \, \phi_{g'}(\boldsymbol{x}) \, dV \\
&\quad + \int_{V_j} w_j(\boldsymbol{x}) \, Q_{0,g}(\boldsymbol{x}) \, dV + \int_{S_j} w_j(\boldsymbol{x}) \, J_g^{b-}(\boldsymbol{x}) \, dS,
\end{aligned}$$

$$\boldsymbol{x} \in V, \quad g = 1, \ldots, G. \tag{62}$$

Using Fick's Law (Eq. 49) and the partial currents (Eq. 54), the final equations are

$$\begin{aligned}
\left(\frac{1-\rho}{4}\right) \left[\int_{S_j} w_j(\boldsymbol{x}) \, \phi_g(\boldsymbol{x}, t) \, dS - 2D_{j,g} \boldsymbol{n} \cdot \int_{S_j} w_j(\boldsymbol{x}) \, \boldsymbol{\nabla}\phi_g(\boldsymbol{x}) \, dS\right] &+ D_{j,g} \int_{V_j} \left[\boldsymbol{\nabla} w_j(\boldsymbol{x})\right] \cdot \left[\boldsymbol{\nabla}\phi_g(\boldsymbol{x})\right] dV \\
&+ \Sigma_{t;j,g} \int_{V_j} w_j(\boldsymbol{x}) \, \phi_g(\boldsymbol{x}) \, dV \\
= \sum_{g'=1}^{G} \Sigma_{s;j,0,g'\to g} \int_{V_j} w_j(\boldsymbol{x}) \, \phi_{g'}(\boldsymbol{x}) \, dV &+ \frac{\chi_{j,g}}{4\pi} \sum_{g'=1}^{G} \nu\Sigma_{f;j,g'} \int_{V_j} w_j(\boldsymbol{x}) \, \phi_{g'}(\boldsymbol{x}) \, dV \\
+ \int_{V_j} w_j(\boldsymbol{x}) \, Q_{0,g}(\boldsymbol{x}) \, dV &+ \int_{S_j} w_j(\boldsymbol{x}) \, J_g^{b-}(\boldsymbol{x}) \, dS,
\end{aligned}$$

$$\boldsymbol{x} \in V, \quad g = 1, \ldots, G. \tag{63}$$

The ρ may be dependent on which boundary is being integrated. If so, the surface integral will be of the form

$$\sum_m \left(\frac{1-\rho_m}{4}\right) \int_{S_{j,m}} w_j(\boldsymbol{x}) \, (\cdot) \, dS. \tag{64}$$

For the interior of the problem, if the discontinuous finite element method is being used, the integral over the boundary current J_g^{b-} instead becomes an integral over the boundary current exiting the neighboring cells. Unlike in DFEM transport methods where only the contribution of upwind cells is taken into account, in the diffusion method there is no concept of upwind or downwind and the incoming current from all of the neighboring cells must be included. For between-cell current, the albedo coefficient will be zero, i.e. $\rho = 0$.

Part III
Iteration methods

6 Operator notation

The steady-state neutron transport equation can be written in operator notation for both the strong and weak forms of the equation. In either case we have the transport operator $\mathcal{L}$, the discrete-to-moment operator $\mathcal{D}$, the moment-to-discrete operator $\mathcal{M}$, the scattering operator $\mathcal{S}$ and the fission operator $\mathcal{F}$. The transport equation can then be written as

$$\mathcal{L}\psi = \mathcal{M}\left(\mathcal{S}+\mathcal{F}\right)\mathcal{D}\psi + s. \tag{65}$$

For the strong form of the equation, we have (from Eq. 19)

$$\left(\mathcal{L}\psi\right)_{n,g,j} = \boldsymbol{\Omega}\cdot\boldsymbol{\nabla}\psi_{n,g} + \Sigma_{t,g}\psi_{n,g}\Big|_{\boldsymbol{x}=\boldsymbol{x}_j}, \tag{66}$$

$$\left(\mathcal{D}\psi\right)^m_{\ell,g,j} = \sum_n Y^m_\ell\left(\boldsymbol{\Omega}_n\right) w_n \psi_{n,g}\Big|_{\boldsymbol{x}=\boldsymbol{x}_j}, \tag{67}$$

$$\left(\mathcal{M}\phi\right)_{n,g,j} = \sum_\ell \frac{2\ell+1}{4\pi}\sum_m Y^m_\ell\left(\boldsymbol{\Omega}_n\right)\phi^m_{\ell,g}\Big|_{\boldsymbol{x}=\boldsymbol{x}_j}, \tag{68}$$

$$\left(\mathcal{S}\phi\right)^m_{\ell,g,j} = \sum_{g'}\Sigma^m_{s,\ell,g'\to g}\phi^m_{\ell,g'}\Big|_{\boldsymbol{x}=\boldsymbol{x}_j}, \tag{69}$$

$$\left(\mathcal{F}\phi\right)^m_{\ell,g,j} = \delta_{\ell,0}\chi_g\sum_{g'}\nu_{g'}\Sigma_{f,g'}\phi^m_{\ell,g'}\Big|_{\boldsymbol{x}=\boldsymbol{x}_j}, \tag{70}$$

$$s = q\Big|_{\boldsymbol{x}=\boldsymbol{x}_j} \tag{71}$$

The weak form of the equation with constant or weighted coefficients (Eq. 26) becomes

$$\left(\mathcal{L}\psi\right)_{n,g,j} = \int_{\boldsymbol{\Omega}_n\cdot\boldsymbol{n}>0}\left(\boldsymbol{\Omega}_n\cdot\boldsymbol{n}\right)\psi_{n,g}w_j dS - \int_{V_j}\psi_{n,g}\left[\boldsymbol{\Omega}\cdot\boldsymbol{\nabla}w_j\right]dV + \Sigma_{t;g,j}\int_{V_j}w_j\psi_{n,g}dV, \tag{72}$$

$$\left(\mathcal{D}\psi\right)^m_{\ell,g,j} = \sum_n Y^m_\ell\left(\boldsymbol{\Omega}_n\right)w_n\psi_{n,g} \tag{73}$$

$$\left(\mathcal{M}\phi\right)_{n,g,j} = \sum_{\ell=0}^{L}\frac{2\ell+1}{4\pi}\sum_{m=-\ell}^{\ell}Y^m_\ell\left(\boldsymbol{\Omega}_n\right)\phi^m_{\ell,g}, \tag{74}$$

$$\left(\mathcal{S}\phi\right)^m_{\ell,g,j} = \sum_{g'=1}^{G}\Sigma_{s;\ell,g'\to g,j}\int_{V_j}w_j\phi^m_{\ell,g'}dV, \tag{75}$$

$$\left(\mathcal{F}\phi\right)^m_{\ell,g,j} = \delta_{\ell,0}\chi_{g,j}\sum_{g'=1}^{G}\nu\Sigma_{f,g',j}\int_{V_j}w_j\phi^0_{0,g'}\left(\boldsymbol{x}\right)dV, \tag{76}$$

$$s_{n,g,j} = \int_{V_j}w_j q_{n,g}dV + \sum_{i=1}^{J}\alpha^b_{i,n,g}\int_{\boldsymbol{\Omega}_n\cdot\boldsymbol{n}<0}\left|\boldsymbol{\Omega}_n\cdot\boldsymbol{n}\right|b_i w_j dS. \tag{77}$$

When we add basis functions, the weak form can also be written as iteration over the coefficients of the solution, which can be solved for instead of the angular flux or its moments. From Eqs. 33 and 34, we have

$$\left(\tilde{\mathcal{L}}\alpha\right)_{n,g,j} = \sum_{i=1}^{J}\left[\int_{\boldsymbol{\Omega}_n\cdot\boldsymbol{n}>0}\left(\boldsymbol{\Omega}_n\cdot\boldsymbol{n}\right)b_i w_j dS - \int_{V_j}b_i\left(\boldsymbol{x}\right)\left[\boldsymbol{\Omega}_n\cdot\boldsymbol{\nabla}w_j\right]dV + \Sigma_{t;g,j}\int_{V_j}b_i w_j dV\right]\alpha_{i,n,g}, \tag{78}$$

$$\left(\tilde{\mathcal{S}}\beta\right)_{\ell,g,j}^{m} = \sum_{g'} \Sigma_{s;\ell,g'\to g,j}^{m} \sum_{i=1}^{J} \beta_{\ell,g',j}^{m} \int_{V_j} b_i w_j dV, \tag{79}$$

$$\left(\tilde{\mathcal{F}}\beta\right)_{\ell,g,j}^{m} = \delta_{\ell,0}\chi_{g,j} \sum_{g'} \nu\Sigma_{f;g',j} \sum_{i=1}^{J} \beta_{i,0,g'}^{0} \int_{V_j} b_i\left(\boldsymbol{x}\right) w_j\left(\boldsymbol{x}\right) dV, \tag{80}$$

$$s_{n,g,j} = \int_{V_j} w_j q_{n,g} dV + \sum_{i=1}^{J} \alpha_{i,n,g}^{b} \int_{\boldsymbol{\Omega}_n\cdot\boldsymbol{n}<0} \left|\boldsymbol{\Omega}_n \cdot \boldsymbol{n}\right| b_i w_j dS, \tag{81}$$

while the definitions of $\mathcal{M}$ and $\mathcal{D}$ remain unchanged. If we define

$$\tilde{\phi}_{\ell,g,j}^{m} = \sum_{i=1}^{J} \beta_{\ell,g',j}^{m} \int_{V_j} b_i\left(\boldsymbol{x}\right) w_j\left(\boldsymbol{x}\right) dV, \tag{82}$$

the scattering and fission operators become

$$\left(\mathcal{S}\beta\right)_{\ell,g,j}^{m} = \sum_{g'} \Sigma_{s;\ell,g'\to g,j}^{m} \tilde{\phi}_{\ell,g',j}^{m}, \tag{83}$$

$$\left(\mathcal{F}\beta\right)_{\ell,g,j}^{m} = \delta_{\ell,0}\chi_{g,j} \sum_{g'} \nu\Sigma_{f;g',j} \tilde{\phi}_{\ell,g',j}, \tag{84}$$

which is in the same form as the strong form of the problem. Thus, if we define

$$\left(\tilde{\mathcal{C}}\beta\right)_{\ell,g,j}^{m} = \sum_{i=1}^{J} \beta_{i,\ell,g'}^{m} \int_{V_j} b_i\left(\boldsymbol{x}\right) w_j\left(\boldsymbol{x}\right) dV, \tag{85}$$

then we can write the system of equations as

$$\tilde{\mathcal{L}}\alpha = \mathcal{M}\left(\mathcal{S}+\mathcal{F}\right)\tilde{\mathcal{C}}\mathcal{D}\alpha + s, \tag{86}$$

after which the operators $\mathcal{M}$, $\mathcal{S}$ and $\mathcal{F}$ and $\mathcal{D}$ are unchanged. Most of the time in finite element methods, the basis functions have the Dirac delta property, which means that the value of the function at the nodes is equal to the value of the corresponding coefficient,

$$\psi\left(\boldsymbol{x}_i\right) = \alpha_i. \tag{87}$$

In these cases, the $\tilde{\mathcal{C}}$ operator would not be needed, as the nodal values of the angular flux directly produce the nodal values for its moments, the scattering source and fission, which are then automatically interpolated in the basis expansion. The addition of the $\tilde{\mathcal{C}}$ operator

- Allows for solution using basis functions without the Dirac delta property,
- Moves the integrals outside of the scattering and fission operator definitions, and
- Prevents spatial information from being destroyed that would then need to be reintroduced by interpolation.

7 Steady-state equation

To solve for the moments of the angular flux instead of the angular flux itself, apply the operator $\mathcal{D}\mathcal{L}^{-1}$ to each side of Eq. 65 to get

$$\phi = \mathcal{D}\mathcal{L}^{-1}M\left(\mathcal{S}+\mathcal{F}\right)\phi + DL^{-1}s.$$

This equation can be used for source (or Richardson) iteration. Gathering the ϕ terms gives

$$\left(\mathcal{I} - \mathcal{D}\mathcal{L}^{-1}\mathcal{M}\left(\mathcal{S}+\mathcal{F}\right)\right)\phi = \mathcal{D}\mathcal{L}^{-1}s,$$

which is a form suitable for solution by Krylov iteration. These equations include the source term, $\mathcal{D}\mathcal{L}^{-1}s$, which includes the contribution of the boundary term and represents the first-flight flux. To handle reflective boundaries, we follow Warsa et. al [1] and use augments to store the outgoing flux at the boundaries for the next iteration. For the source term, this means iterating on the source and its reflected component until convergence is reached. Once convergence is reached, the augments in the source term are zeroed out (since the first-flight flux already includes the boundary source). The terms $\mathcal{D}$, $\mathcal{M}$, $\mathcal{S}$ and $\mathcal{F}$ ignore the augments, which are only used inside $\mathcal{L}^{-1}$. The identity operator is still an identity operator for the augments. Mathematically, the augments do the following:

$$\phi \rightarrow \begin{bmatrix} \phi \\ \psi_R \end{bmatrix},$$
$$\mathcal{D} \rightarrow \begin{bmatrix} \mathcal{D} & 0 \\ 0 & \mathcal{I}_R \end{bmatrix},$$
$$\mathcal{M} \rightarrow \begin{bmatrix} \mathcal{M} & 0 \\ 0 & \mathcal{I}_R \end{bmatrix},$$
$$\mathcal{S} \rightarrow \begin{bmatrix} \mathcal{S} & 0 \\ 0 & \mathcal{I}_R \end{bmatrix},$$
$$s \rightarrow \begin{bmatrix} s \\ 0 \end{bmatrix}.$$

Optionally, another two operators can be added that represent adding the augments into the angular flux and storing the reflected flux after the action of $\mathcal{L}^{-1}$. In this code, these two operators are included in the $\mathcal{L}^{-1}$ operator.

8 k-eigenvalue equation

The k-eigenvalue equation can be written in operator notation as

$$\mathcal{L}\psi = \mathcal{M}\left(\mathcal{S} + \frac{1}{k}\mathcal{F}\right)\mathcal{D}\psi, \tag{88}$$

where the operators are defined the same as in the steady-state case and the eigenvalue is k. This can be written in moment form as

$$\phi = D\mathcal{L}^{-1}\mathcal{M}\left(\mathcal{S} + \frac{1}{k}\mathcal{F}\right)\phi, \tag{89}$$

which represents fixed point iteration. After each iteration, the eigenvalue is updated as

$$k^{(\ell+1)} = \frac{\left\|\mathcal{F}\phi^{(\ell+1)}\right\|}{\left\|\frac{1}{k^{(\ell)}}\mathcal{F}\phi^{(\ell)} - \mathcal{S}\left(\phi^{\ell+1} - \phi^{\ell}\right)\right\|}.$$

To derive the equations for power iteration, isolate the fission term and the invert the equation onto it, which gives

$$\phi = \left(\mathcal{I} - \mathcal{D}\mathcal{L}^{-1}\mathcal{M}\mathcal{S}\right)^{-1}\mathcal{D}\mathcal{L}^{-1}\mathcal{M}\frac{1}{k}\mathcal{F}\phi.$$

For power iteration, the eigenvalue is updated after each iteration as

$$k^{(\ell+1)} = \frac{\left\|\mathcal{F}\phi^{(\ell+1)}\right\|}{\left\|\frac{1}{k^{(\ell)}}\mathcal{F}\phi^{(\ell)}\right\|}.$$

Finally, for Krylov eigenvalue iteration, isolate the eigenvalue in the equation to get

$$\left(\mathcal{I} - \mathcal{D}\mathcal{L}^{-1}\mathcal{M}\mathcal{S}\right)^{-1} D\mathcal{L}^{-1}\mathcal{M}\mathcal{F}\phi = k\phi.$$

For power and Krylov eigenvalue iteration, the inverse of the operator $\left(\mathcal{I} - \mathcal{D}\mathcal{L}^{-1}\mathcal{M}\mathcal{S}\right)^{-1}$ is needed, which is roughly the action needed when inverting the steady-state operator. This inverse can be performed by a standard Krylov solver such as GMRES. The full system can be solved with a Krylov eigensolver that admits asymmetric matrices, such as Block Krylov-Schur or Generalized Davidson.

9 Time-dependent equation (not yet implemented)

Define

$$\mathcal{T}\psi_{j,n,g} = \frac{\psi_{j,n,g}}{2\Delta t}.$$

Then Crank-Nicolson can be written as

$$\mathcal{T}\psi^{(\ell+1)} - \mathcal{T}\psi^{(\ell)} = \left[\mathcal{M}\left(\mathcal{S}+\mathcal{F}\right)\mathcal{D} - \mathcal{L}\right]\psi^{(\ell+1)} + \left[\mathcal{M}\left(\mathcal{S}+\mathcal{F}\right)\mathcal{D} - \mathcal{L}\right]\psi^{(\ell)} + s^{(\ell+1)} + s^{(\ell)}$$

Define the $\mathcal{L}_+$ and $\mathcal{L}_-$ operators as

$$\mathcal{L}_+ = \mathcal{L} + \mathcal{T},$$
$$\mathcal{L}_- = \mathcal{L} - \mathcal{T},$$

to get

$$\mathcal{L}_+\psi^{(\ell+1)} = \mathcal{M}\left(\mathcal{S}+\mathcal{F}\right)\mathcal{D}\psi^{(\ell+1)} + \left[\mathcal{M}\left(\mathcal{S}+\mathcal{F}\right)\mathcal{D} - \mathcal{L}_-\right]\psi^{(\ell)} + s^{(\ell+1)} + s^{(\ell)}.$$

The problem can then be written in the same form as a fixed-source problem,

$$\phi^{(\ell+1)} = \mathcal{D}\mathcal{L}_+^{-1}\mathcal{M}\left(\mathcal{S}+\mathcal{F}\right)\phi^{(\ell+1)} + \mathcal{D}\mathcal{L}_+^{-1}\tilde{s}^{(\ell+1)},$$

with

$$\tilde{s}^{(\ell+1)} = \left[\mathcal{M}\left(\mathcal{S}+\mathcal{F}\right)\mathcal{D} - \mathcal{L}_-\right]\psi^{(\ell)} + s^{(\ell+1)} + s^{(\ell)}.$$

Part IV
Meshless methods

10 Radial basis functions

10.1 Introduction to radial basis functions

The value of a radial basis function (RBF) depends only on the distance traversed by the input vector,

$$\Gamma(\boldsymbol{x}) = \Gamma(\|\boldsymbol{x}\|) = \Gamma(r),$$

regardless of the number of dimensions. Examples of radial basis functions include the Gaussian (GA), multiquadric (MQ) and inverse multiquadric (IMQ),

$$\text{GA}: \qquad \Gamma(r) = e^{-(r)^2}, \tag{90}$$

$$\text{MQ}: \qquad \Gamma(r) = \sqrt{1+(r)^2}, \tag{91}$$

$$\text{IMQ}: \qquad \Gamma(r) = \frac{1}{\sqrt{1+(r)^2}}. \tag{92}$$

RBFs can act as a functional basis,

$$f(\boldsymbol{x}) = \sum_i a_i \Gamma_i(\boldsymbol{x}), \tag{93}$$

where

$$\Gamma_i(\boldsymbol{x}) = \Gamma(\epsilon_i \|\boldsymbol{x} - \boldsymbol{x}_i\|), \tag{94}$$

where ϵ_i is the shape parameter, which controls how quickly the RBF increases or decreases away from the center, and $\boldsymbol{x}_i$ is the location of the center of the basis function.

For interpolation, a pointwise or an integral method can be used. For pointwise interpolation, given certain sample points located at $\boldsymbol{x}_i$, equations are

$$\begin{bmatrix} \Gamma_1(\boldsymbol{x}_1) & \Gamma_2(\boldsymbol{x}_1) & \cdots & \Gamma_I(\boldsymbol{x}_1) \\ \Gamma_1(\boldsymbol{x}_2) & \Gamma_2(\boldsymbol{x}_2) & \cdots & \Gamma_I(\boldsymbol{x}_2) \\ \vdots & \vdots & \vdots & \vdots \\ \Gamma_1(\boldsymbol{x}_I) & \Gamma_2(\boldsymbol{x}_I) & \cdots & \Gamma_I(\boldsymbol{x}_I) \end{bmatrix} \begin{bmatrix} a_1 \\ a_2 \\ \vdots \\ a_I \end{bmatrix} = \begin{bmatrix} f(\boldsymbol{x}_1) \\ f(\boldsymbol{x}_2) \\ \vdots \\ f(\boldsymbol{x}_I) \end{bmatrix}. \tag{95}$$

The interpolant can then be evaluated using Eq. 93 using the calculated a_i values. For weak interpolation using the Galerkin method, these functions are instead

$$\begin{bmatrix} \int_V \tilde{\Gamma}_1(\boldsymbol{x})\Gamma_1(\boldsymbol{x})\,dV & \int_V \tilde{\Gamma}_1(\boldsymbol{x})\Gamma_2(\boldsymbol{x})\,dV & \cdots & \int_V \tilde{\Gamma}_1(\boldsymbol{x})\Gamma_I(\boldsymbol{x})\,dV \\ \int_V \tilde{\Gamma}_2(\boldsymbol{x})\Gamma_1(\boldsymbol{x})\,dV & \int_V \tilde{\Gamma}_2(\boldsymbol{x})\Gamma_2(\boldsymbol{x})\,dV & \cdots & \int_V \tilde{\Gamma}_2(\boldsymbol{x})\Gamma_I(\boldsymbol{x})\,dV \\ \vdots & \vdots & \vdots & \vdots \\ \int_V \tilde{\Gamma}_I(\boldsymbol{x})\Gamma_1(\boldsymbol{x})\,dV & \int_V \tilde{\Gamma}_I(\boldsymbol{x})\Gamma_2(\boldsymbol{x})\,dV & \cdots & \int_V \tilde{\Gamma}_I(\boldsymbol{x})\Gamma_I(\boldsymbol{x})\,dV \end{bmatrix} \begin{bmatrix} a_1 \\ a_2 \\ \vdots \\ a_I \end{bmatrix} = \begin{bmatrix} \int_V \tilde{\Gamma}_1(\boldsymbol{x})f(\boldsymbol{x})\,dV \\ \int_V \tilde{\Gamma}_2(\boldsymbol{x})f(\boldsymbol{x})\,dV \\ \vdots \\ \int_V \tilde{\Gamma}_I(\boldsymbol{x})f(\boldsymbol{x})\,dV \end{bmatrix}, \tag{96}$$

where the $\tilde{\Gamma}$ are the weight functions (which would be the same as the basis functions in the Galerkin method). In practice, the weak form would not be used for interpolation since the function $f(\boldsymbol{x})$ would need to be known at all points in the domain a priori, which would defeat the purpose of interpolation. This second method is mentioned to show how the Galerkin method could work when solving a differential

equation. Fig. 2 shows the interpolation results. The basis (and weight, where applicable) functions are a set of Gaussian basis functions over a slab of length $L = 1$ with a constant spacing of $\Delta x = L/I$ and shape parameters of $\epsilon_i = 1/\Delta x$. The unscaled basis functions are all identical. Once the interpolation is completed, the scaled basis functions show how each of the basis functions contributes individually to the interpolant. The weak interpolant does not perform significantly better than the strong interpolant in this case. The weak interpolant near the boundary is poor due to the integral nature of the interpolantion. The interpolant struggles where the function is not smooth (near the discontinuities in the first derivative).

The Gaussian functions fail to exactly reproduce a constant and a linear function correctly, which means they do not satisfy the Eq. 30. This means that they are not ideal for use as weight functions in a Petrov-Galerkin method as they will not exactly enforce conservation. Fig. 1 shows the attempted fit to a constant and to a linear function. The error is nonzero except at the interpolation points.

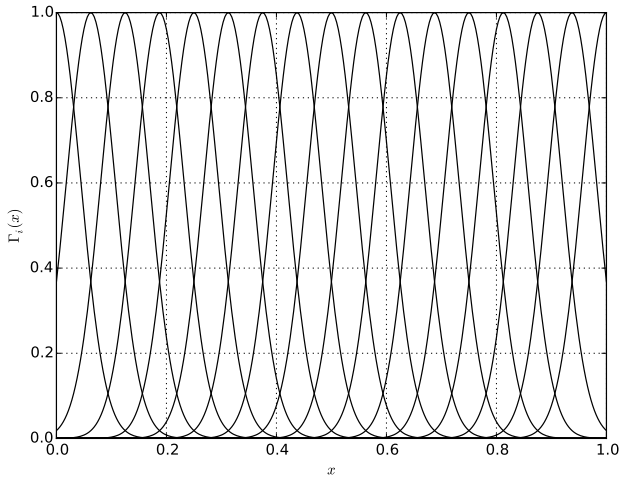

(a) Basis function set, $\Gamma_i(\boldsymbol{x})$

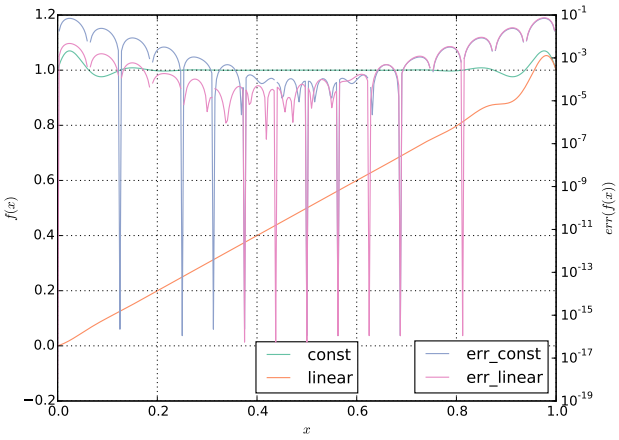

(b) Interpolation of a constant and a linear function

Figure 1: Gaussian basis with 17 points

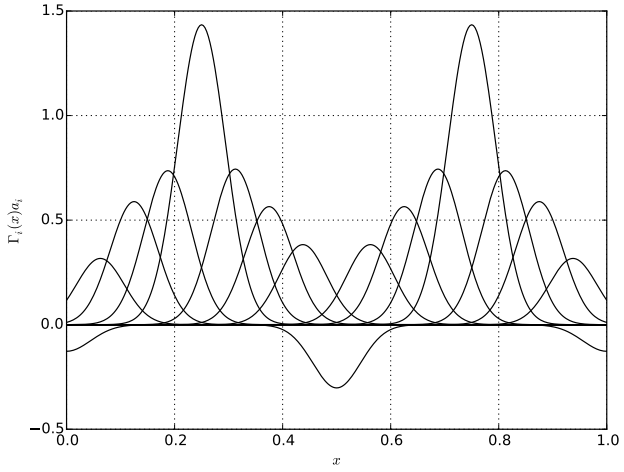

(a) Scaled basis functions for the pointwise interpolation, $a_i\Gamma_i(\boldsymbol{x})$

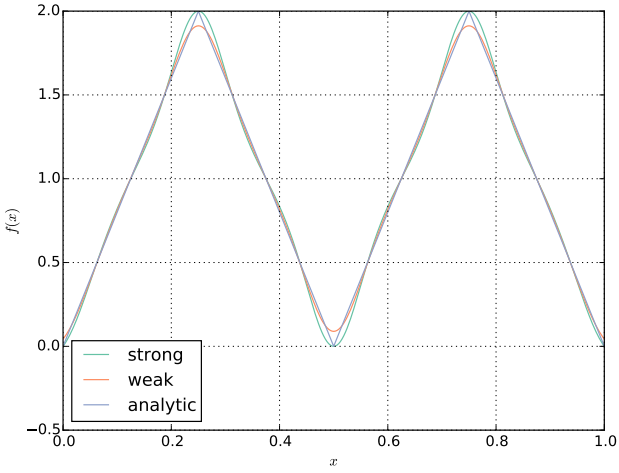

(b) Interpolation result

Figure 2: Interpolation of a sawtooth wave using 17 identical Gaussian basis and weight functions

10.2 Localization of basis functions

11 Moving least squares

The moving least squares method is one meshless approach to basis functions that retains the ability to represent a certain order of polynomials exactly. The idea is to minimize error of the function $f(\boldsymbol{x})$ with respect to some values f_i in a least-squares sense.

EXPLAIN MINIMIZATION, DERIVE METHOD

Start with a basis of m polynomials and n points. The shape functions themselves are simply

$$\phi_i(\boldsymbol{x}) = \boldsymbol{p}^\top(\boldsymbol{x}) \boldsymbol{A}^{-1}(\boldsymbol{x}) \boldsymbol{B}_i(\boldsymbol{x}),$$

with

$$\boldsymbol{p}^\top(\boldsymbol{x}) = \{p_0(\boldsymbol{x}), p_1(\boldsymbol{x}), p_2(\boldsymbol{x}), \dots, p_m(\boldsymbol{x})\} = \{1, x, y, z, xy, xz, yz, x^2, y^2, z^2, \dots\},$$
$$\boldsymbol{A}(\boldsymbol{x}) = \sum_{i=1}^{n} W_i(\boldsymbol{x}) \boldsymbol{p}(\boldsymbol{x}_i) \boldsymbol{p}^\top(\boldsymbol{x}_i),$$
$$\boldsymbol{B}_i(\boldsymbol{x}) = w_i(\boldsymbol{x}) \boldsymbol{p}(\boldsymbol{x}_i),$$

where $w_i(\boldsymbol{x})$ is a weighting function centered at the point $\boldsymbol{x}_i$. The derivatives are

$$\frac{\partial \phi_i(\boldsymbol{x})}{\partial x_j} = \frac{\partial \boldsymbol{p}^\top(\boldsymbol{x})}{\partial x_j} \boldsymbol{A}^{-1}(\boldsymbol{x}) \boldsymbol{B}_i(\boldsymbol{x}) + \boldsymbol{p}^\top(\boldsymbol{x}) \frac{\partial \boldsymbol{A}^{-1}(\boldsymbol{x})}{\partial x_j} \boldsymbol{B}_i(\boldsymbol{x}) + \boldsymbol{p}^\top(\boldsymbol{x}) \boldsymbol{A}^{-1}(\boldsymbol{x}) \frac{\partial \boldsymbol{B}_i(\boldsymbol{x})}{\partial x_j},$$

where

$$\frac{\partial \boldsymbol{B}_i}{\partial x_j} = \frac{\partial w_i(\boldsymbol{x})}{\partial x_j} \boldsymbol{p}(\boldsymbol{x}_i),$$
$$\frac{\partial \boldsymbol{A}^{-1}(\boldsymbol{x})}{\partial x_j} = -\boldsymbol{A}^{-1}(\boldsymbol{x}) \frac{\partial \boldsymbol{A}(\boldsymbol{x})}{\partial x_j} \boldsymbol{A}^{-1}(\boldsymbol{x}),$$
$$\frac{\partial \boldsymbol{A}(\boldsymbol{x})}{\partial x_j} = \sum_{i=1}^{n} \frac{\partial \hat{W}_i(\boldsymbol{x})}{\partial x_j} \boldsymbol{p}(\boldsymbol{x}_i) \boldsymbol{p}^\top(\boldsymbol{x}_i).$$

Figure 3 shows the MLS basis functions, which are not symmetric about the center as are RBFs. The defining feature of the MLS functions is the ability to exactly represent polynomials up to a defined order. In this case, only a linear basis is used. As is evident, the MLS basis functions are approximating the constant and linear functions to machine precision.

Like RBFs, MLS basis functions are not able to easily represent large discontinuities in the solution. Figure 4 shows the attempt at interpolating a square wave using MLS basis and weight functions without a sufficient number to finely resolve the discontinuities. As in the RBF case, the weak form does not have the Dirac delta property at the boundary, i.e. the value of the interpolant at the boundary does not equal the boundary condition.

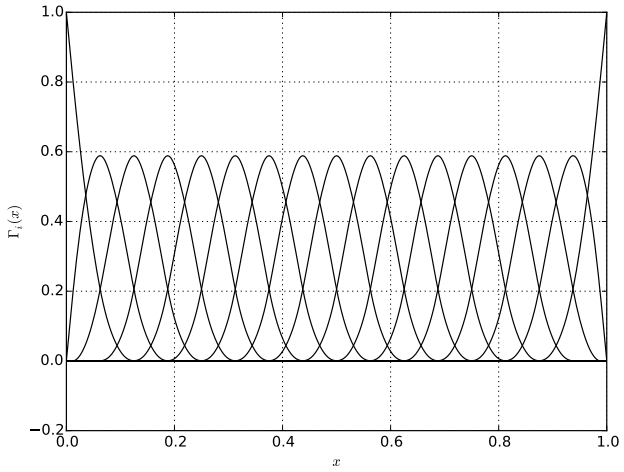

(a) Basis function set, $\Gamma_i(\boldsymbol{x})$

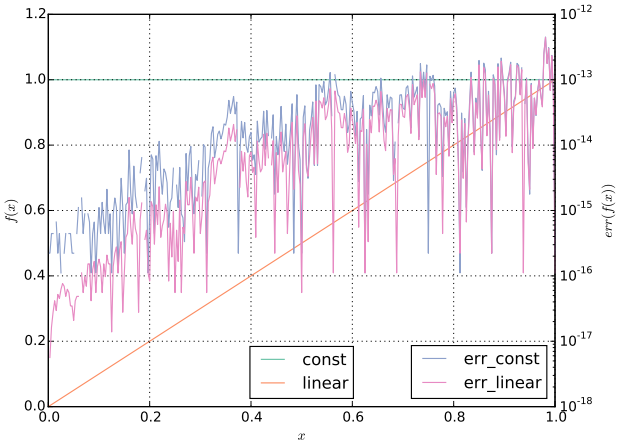

(b) Interpolation of a constant and a linear function

Figure 3: Linear MLS basis with 17 points

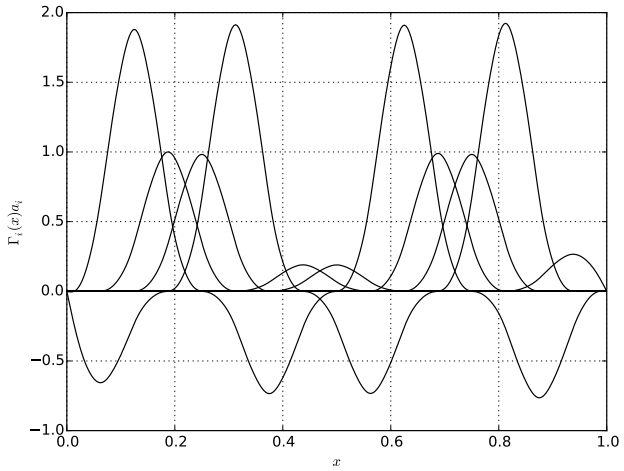

(a) Scaled basis functions for the pointwise interpolation, $a_i\Gamma_i(\boldsymbol{x})$

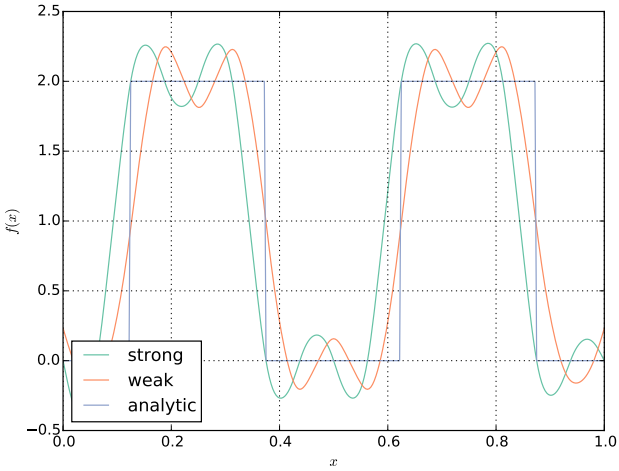

(b) Interpolation result

Figure 4: Interpolation of a square wave using 17 MLS basis and weight functions

Part V
Math

12 Integrals in weak forms

For both the diffusion and the transport equation, integrals of the form

$$\int_V w(\boldsymbol{x})\,\boldsymbol{\nabla}\cdot\boldsymbol{F}(\boldsymbol{x})\,dV \tag{97}$$

must be done, which require either the chain rule,

$$\boldsymbol{\nabla}\cdot(w(\boldsymbol{x})\,\boldsymbol{F}(\boldsymbol{x})) = [\boldsymbol{\nabla}w(\boldsymbol{x})]\cdot\boldsymbol{F}(\boldsymbol{x}) + w(\boldsymbol{x})\,\boldsymbol{\nabla}\cdot\boldsymbol{F}(\boldsymbol{x}), \tag{98}$$

or integration by parts to get

$$\int_V w(\boldsymbol{x})\,\boldsymbol{\nabla}\cdot\boldsymbol{F}(\boldsymbol{x})\,dV = \int_V \boldsymbol{\nabla}\cdot(w(\boldsymbol{x})\,\boldsymbol{F}(\boldsymbol{x}))\,dV - \int_V [\boldsymbol{\nabla}w(\boldsymbol{x})]\cdot\boldsymbol{F}(\boldsymbol{x})\,dV. \tag{99}$$

Then using the divergence theorem gives

$$\int_V \boldsymbol{\nabla}\cdot(w(\boldsymbol{x})\,\boldsymbol{F}(\boldsymbol{x}))\,dV = \int_S w(\boldsymbol{x})\,(\boldsymbol{F}(\boldsymbol{x})\cdot\boldsymbol{n})\,dS, \tag{100}$$

or in whole,

$$\int_V w(\boldsymbol{x})\,\boldsymbol{\nabla}\cdot\boldsymbol{F}(\boldsymbol{x})\,dV = \int_S w(\boldsymbol{x})\,(\boldsymbol{F}(\boldsymbol{x})\cdot\boldsymbol{n})\,dS - \int_V [\boldsymbol{\nabla}w(\boldsymbol{x})]\cdot\boldsymbol{F}(\boldsymbol{x})\,dV. \tag{101}$$

For the transport equation,

$$\boldsymbol{F}(\boldsymbol{x}) = \boldsymbol{\Omega}\psi(\boldsymbol{x},\boldsymbol{\Omega}),$$

so the integral becomes

$$\int_V w(\boldsymbol{x})\,\boldsymbol{\Omega}\cdot\boldsymbol{\nabla}\psi(\boldsymbol{x},\boldsymbol{\Omega})\,dV = \int_S w(\boldsymbol{x})\,(\boldsymbol{\Omega}\cdot\boldsymbol{n})\,\psi(\boldsymbol{x},\boldsymbol{\Omega})\,dS - \int_V [\boldsymbol{\Omega}\cdot\boldsymbol{\nabla}w(\boldsymbol{x})]\,\psi(\boldsymbol{x},\boldsymbol{\Omega})\,dV. \tag{102}$$

The diffusion equation has

$$\boldsymbol{F}(\boldsymbol{x}) = D(\boldsymbol{x})\,\boldsymbol{\nabla}\phi(\boldsymbol{x}),$$

so the volume integral becomes

$$\int_V w(\boldsymbol{x})\,\boldsymbol{\nabla}\cdot D(\boldsymbol{x})\,\boldsymbol{\nabla}\phi(\boldsymbol{x})\,dV = \int_S w(\boldsymbol{x})\,D(\boldsymbol{x})\,[(\boldsymbol{\nabla}\cdot\boldsymbol{n})\,\phi(\boldsymbol{x})]\,dS - \int_V D(\boldsymbol{x})\,[\boldsymbol{\nabla}w(\boldsymbol{x})]\cdot[\boldsymbol{\nabla}\phi(\boldsymbol{x})]\,dV. \tag{103}$$

13 Legendre polynomials

14 Spherical harmonics

Part VI
Geometry

15 Quadrature sets

The following equations convert from various geometries to an integral of the form

$$\int_{-1}^{1} f(\xi)\, d\xi = \sum_i w_i f(\xi_i),$$

where the ordinates ξ_i and weights w_i are some 1D quadrature scheme such as the Gauss-Legendre ordinates. All the quadratures map the calculated quadrature back to Cartesian coordinates.

15.1 Cartesian 1D

To convert from $x \in [x_1, x_2]$ to $\xi \in [-1, 1]$, use

$$x(\xi) = \frac{1-\xi}{2} x_1 + \frac{1+\xi}{2} x_2$$

to get

$$dx = \frac{x_2 - x_1}{2} d\xi.$$

The integral then becomes

$$\begin{aligned} \int_{x_1}^{x_2} f(x)\, dx &= \frac{x_2 - x_1}{2} \int_{-1}^{1} f(x(\xi))\, d\xi \\ &= \frac{x_2 - x_1}{2} \sum_i w_i f(x(\xi_i)). \end{aligned}$$

15.2 Cartesian 2D

To convert from $x \in [x_1, x_2]$ and $y \in [y_1, y_2]$ to $\xi \in [-1, 1]$ and $\eta \in [-1, 1]$, use similar rules to the 1D case,

$$\begin{aligned} x(\xi) &= \frac{1-\xi}{2} x_1 + \frac{1+\xi}{2} x_2, \\ y(\eta) &= \frac{1-\eta}{2} y_1 + \frac{1-\eta}{2} y_2, \end{aligned}$$

to get the independent differentials,

$$\begin{aligned} dx &= \frac{x_2 - x_1}{2} d\xi, \\ dy &= \frac{y_2 - y_1}{2} d\eta. \end{aligned}$$

The integral is

$$\begin{aligned} \int_{x_1}^{x_2} \int_{y_1}^{y_2} f(x, y)\, dx dy &= \frac{x_2 - x_1}{2} \frac{y_2 - y_1}{2} \int_{-1}^{1} \int_{-1}^{1} f(x(\xi), y(\eta))\, d\xi d\eta \\ &= \frac{x_2 - x_1}{2} \frac{y_2 - y_1}{2} \sum_{i,j} w_i w_j f(x(\xi_i), y(\eta_j)). \end{aligned}$$

15.3 Cylindrical 2D

Use

$$r = \frac{1-\xi}{2} r_1 + \frac{1+\xi}{2} r_2,$$
$$\theta = \frac{1-\eta}{2} \theta_1 + \frac{1+\eta}{2} \theta_2,$$

where $\theta \in [0, 2\pi]$ and $r \in [0, R]$, which has the differentials

$$dr = \frac{r_2 - r_1}{2} d\xi,$$
$$d\theta = \frac{\theta_2 - \theta_1}{2} d\eta.$$

The conversion to Cartesian coordinates is

$$x(r, \theta) = x_0 + r\cos\theta,$$
$$y(r, \theta) = y_0 + r\sin\theta,$$

where $\boldsymbol{x}_0$ is the location of the center of the cylinder. Then the cylindrical-geometry integral is

$$\begin{aligned}\int_{\theta_1}^{\theta_2} \int_{r_1}^{r_2} f(x(r,\theta), y(r,\theta)) \, r dr d\theta &= \frac{r_2 - r_1}{2} \frac{\theta_2 - \theta_1}{2} \int_{-1}^{1} \int_{-1}^{1} f(x(r(\xi), \theta(\eta)), y(r(\xi), \theta(\eta))) \, r(\xi) \, d\xi d\eta \\ &= \frac{r_2 - r_1}{2} \frac{\theta_2 - \theta_1}{2} \sum_{i,j} f(x(r(\xi_i), \theta(\eta_j)), y(r(\xi_i), \theta(\eta_j))) \, r(\xi).\end{aligned}$$

15.4 Spherical 3D

For the 3D spherical-geometry integral, we use

$$r = \frac{1-\xi}{2} r_1 + \frac{1+\xi}{2} r_2,$$
$$\theta = \frac{1-\eta}{2} \theta_1 + \frac{1+\eta}{2} \theta_2,$$
$$\phi = \frac{1-\zeta}{2} \phi_1 + \frac{1+\zeta}{2} \phi_2,$$

where $r \in [0, r]$, $\theta \in [0, 2\pi]$, $\phi \in [0, \pi]$. The differentials are

$$dr = \frac{r_2 - r_1}{2} d\xi,$$
$$d\theta = \frac{\theta_2 - \theta_1}{2} d\eta,$$
$$d\phi = \frac{\phi_2 - \phi_1}{2} d\zeta.$$

The conversion to Cartesian coordinates is

$$x(r, \theta, \phi) = x_0 + r\cos\theta\sin\phi,$$
$$y(r, \theta, \phi) = y_0 + r\sin\theta\sin\phi,$$
$$z(r, \theta, \phi) = z_0 + r\cos\phi,$$

where $\boldsymbol{x}_0$ is the location of the center of the sphere. Then the integral is

$$\int_0^{\pi} \int_0^{2\pi} \int_0^{r} f(x(r,\theta,\phi), y(r,\theta,\phi), z(r,\phi)) \, r^2 \sin\phi dr d\theta d\phi$$

$$= \frac{r_2 - r_1}{2}\frac{\theta_2 - \theta_1}{2}\frac{\phi_2 - \phi_1}{2}\iiint_{-1}^{1} f\left(x\left(r\left(\xi\right),\theta\left(\eta\right),\phi\left(\zeta\right)\right), y\left(r\left(\xi\right),\theta\left(\eta\right),\phi\left(\zeta\right)\right), z\left(r\left(\xi\right),\phi\left(\zeta\right)\right)\right) r^2\left(\xi\right)\sin\phi\left(\zeta\right) dr d\theta d\phi$$

$$= \frac{r_2 - r_1}{2}\frac{\theta_2 - \theta_1}{2}\frac{\phi_2 - \phi_1}{2}\sum_{i,j,k} f\left(x\left(r\left(\xi_i\right),\theta\left(\eta_j\right),\phi\left(\zeta_k\right)\right), y\left(r\left(\xi_i\right),\theta\left(\eta_j\right),\phi\left(\zeta_k\right)\right), z\left(r\left(\xi_i\right),\phi\left(\zeta_k\right)\right)\right) r^2\left(\xi_i\right)\sin\phi\left(\zeta_k\right) dr d\theta d\phi.$$

15.5 Lens in 2D

For a lens, we have the intersection of two circles as the region of integration. In all cases, we will map the two circles into a simple coordinate system and then rotate/translate the ordinates back into the original coordinates. There are three different cases to be considered, which can be seen in Fig. 5. For the third case, we can use a simple cylindrical quadrature. For the first two, different quadratures must be used.

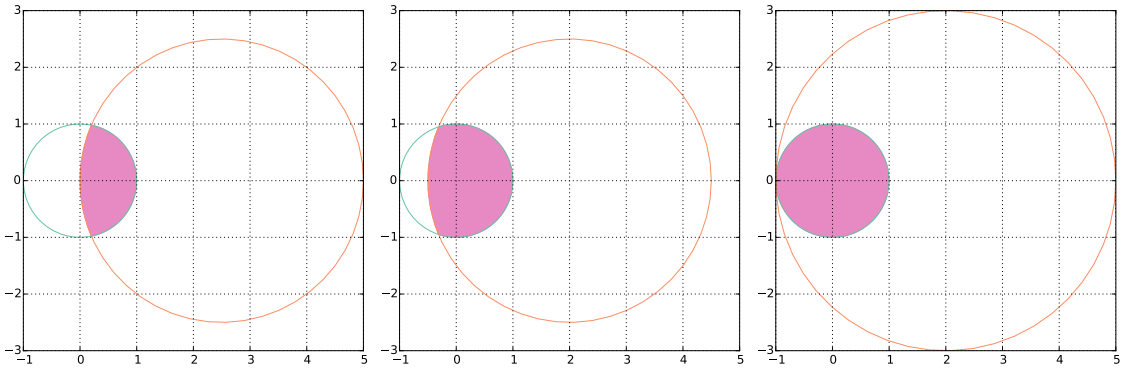

Figure 5: Three lens cases: a standard lens, a non-standard lens, and a full circle

15.5.1 Simple lens

Let the simplified coordinate system $\tilde{x}$, $\tilde{y}$ be defined by

$$\begin{bmatrix} x \\ y \end{bmatrix} = \begin{bmatrix} x_1 \\ y_1 \end{bmatrix} + \frac{1}{d}\begin{bmatrix} \Delta x & -\Delta y \\ \Delta y & \Delta x \end{bmatrix}\begin{bmatrix} \tilde{x} \\ \tilde{y} \end{bmatrix},$$

where the distance between the basis functions is

$$\Delta x = x_2 - x_1,$$
$$\Delta y = y_2 - y_1,$$
$$d = \sqrt{\Delta x^2 + \Delta y^2}.$$

This describes a coordinate system with the first circle centered at the origin and the second circle a distance d away in the $+\hat{x}$ direction. Then in the new coordinate system, we can write the circle equations as

$$x^2 + y^2 = r_1^2,$$
$$\left(x - d\right)^2 + y^2 = r_2^2.$$

The intercepts of these two circles are

$$\tilde{x}_{int} = \frac{d^2 + r_1^2 - r_2^2}{2d},$$
$$\tilde{y}_{int} = \pm\frac{\sqrt{2d^2\left(r_1^2 + r_2^2\right) - \left(r_1^2 - r_2^2\right)^2 - d^4}}{2d}.$$

If we define

$$\tilde{x}_{min}\left(\tilde{y}\right) = d - \sqrt{r_2^2 - \tilde{y}^2},$$
$$\tilde{x}_{max}\left(\tilde{y}\right) = \sqrt{r_1^2 - \tilde{y}^2},$$

then our integral over the lens is of the form

$$\int_{-\tilde{y}_{int}}^{\tilde{y}_{int}} \int_{\tilde{x}_{min}(\tilde{y})}^{\tilde{x}_{max}(\tilde{y})} f\left(\tilde{x}, \tilde{y}\right) dxdy,$$

which can be converted to $\xi \in [-1, 1]$ and $\eta \in [-1, 1]$ using

$$x = \frac{\tilde{x}_{max}\left(\tilde{y}\left(\eta\right)\right) - \tilde{x}_{min}\left(\tilde{y}\left(\eta\right)\right)}{2}\xi + \frac{\tilde{x}_{max}\left(\tilde{y}\left(\eta\right)\right) + \tilde{x}_{min}\left(\tilde{y}\left(\eta\right)\right)}{2},$$
$$\tilde{y} = \tilde{y}_{int}\eta.$$

The Jacobian determinant for this is

$$\begin{aligned} J &= \begin{vmatrix} \frac{d\tilde{x}}{d\xi} & \frac{d\tilde{x}}{d\eta} \\ \frac{d\tilde{y}}{d\xi} & \frac{d\tilde{y}}{d\eta} \end{vmatrix} \\ &= \left(\frac{\tilde{x}_{max}\left(\tilde{y}\left(\eta\right)\right) - \tilde{x}_{min}\left(\tilde{y}\left(\eta\right)\right)}{2}\right)\tilde{y}_{int}, \end{aligned}$$

after which the integral becomes

$$\int_{-1}^{1}\int_{-1}^{1} f\left(\tilde{x}\left(\xi, \eta\right), \tilde{y}\left(\eta\right)\right)\left(\frac{\tilde{x}_{max}\left(\tilde{y}\left(\eta\right)\right) - \tilde{x}_{min}\left(\tilde{y}\left(\eta\right)\right)}{2}\right)\tilde{y}_{int}d\xi d\eta.$$

15.5.2 Non-standard lens

If we assume that the first circle with r_1 has the smaller radius ($r_1 < r_2$) and the $\tilde{x}$ intercept is past the center of this circle, then the integral is identical to the standard lens except for the definitions

$$\tilde{x}_{min}\left(\tilde{y}\right) = \begin{cases} d - \sqrt{r_2^2 - \tilde{y}^2}, & |\tilde{y}| \leq \tilde{y}_{int}, \\ -\sqrt{r_1^2 - \tilde{y}^2}, & \text{otherwise}, \end{cases}$$
$$\tilde{x}_{max}\left(y\right) = \sqrt{r_1^2 - \tilde{y}^2}.$$

If $r_2 > r_1$, then the definitions become

$$\tilde{x}_{min}\left(\tilde{y}\right) = d - \sqrt{r_2^2 - \tilde{y}^2},$$
$$\tilde{x}_{max}\left(\tilde{y}\right) = \begin{cases} \sqrt{r_1^2 - \tilde{y}^2}, & |\tilde{y}| \leq \tilde{y}_{int}, \\ d + \sqrt{r_2^2 - \tilde{y}^2}, & \text{otherwise}. \end{cases}$$

15.6 Quadratures near boundaries

Near boundaries, the most important thing is that the quadrature not extend past the boundary. Since the functions we're integrating fall off away from the center, they're smooth even as they become zero. However, if we include quadrature points past the boundary (and artificially set the weights of these quadrature points to zero), the function we're integrating is no longer smooth, which means that the quadratures will no longer behave ideally.

One easy-to-derive quadrature for use near boundaries is the integration over a cylinder with Cartesian limits $x_{min,max}$ and $y_{min,max}$. For this, we create an array of x points with $x \in [\max(x_0 - r, x_{min}), \min(x_0 + r, x_{max})]$ and then integrate in y between the top and bottom of the circle at the point x, taking into account the y intercepts to get $y \in \left[\max\left(y_0 - \sqrt{r^2 - x^2}, y_{min}\right), \min\left(y_0 + \sqrt{r^2 - x^2}, y_{max}\right)\right]$.

Quadratures for lenses that intersect boundaries are possible but not practical, particularly when going to 3D cases with the intersection of a basis function, weight function and up to three planes that make up a corner. For these cases, using a Cartesian or other quadrature that extends beyond the area where the functions have gone to zero but tightly holds to the boundary works well.

16 Solid geometry

16.1 Shape-specific values

For each surface in a constructive solid geometry, the following information is needed to run a particle simulation:

- The normal vector of the surface at each point on the surface,
- The distance to intersection and point of intersection of a particle incident on the surface, and
- Whether a particle is positive or negative from a surface (which can be arbitrarily defined).

These quantities are calculated below for a plane, a cylinder and a sphere, all with arbitrary position and orientation.

16.1.1 Plane

The general equation for a plane with normal vector $\boldsymbol{n}$ is

$$(\boldsymbol{x} - \boldsymbol{x}_0) \cdot \boldsymbol{n} = 0. \tag{104}$$

Let the particle position be

$$\boldsymbol{x}_p(s) = \boldsymbol{g}_0 + \boldsymbol{g}_1 s \tag{105}$$

and plug it in. Solving for s gives

$$s = \frac{(\boldsymbol{x}_0 - \boldsymbol{g}_0) \cdot \boldsymbol{n}}{\boldsymbol{g}_1 \cdot \boldsymbol{n}}. \tag{106}$$

This is the distance to intersection. The point of intersection can be found by advancing the particle by distance s. To find the geometric relationship between a particle and a plane, we have

$$\boldsymbol{n} \cdot (\boldsymbol{x} - \boldsymbol{x}_0) \begin{cases} > 0, & \text{positive,} \\ < 0, & \text{negative,} \\ = 0, & \text{coincident.} \end{cases}$$

16.1.2 Cylinder

Begin with the equation for a cylinder with the centerline having an axis in direction $\boldsymbol{\Omega}$ that runs through the point $\boldsymbol{x}$. The equation for this cylinder is

$$\left\|\boldsymbol{x} - \boldsymbol{x}_0 - \boldsymbol{\Omega} \cdot (\boldsymbol{x} - \boldsymbol{x}_0)\, \boldsymbol{\Omega}\right\|^2 = r^2.$$

If we again define the particle position as

$$\boldsymbol{x}_p(s) = \boldsymbol{g}_0 + \boldsymbol{g}_1 s, \tag{107}$$

then we get

$$\|\boldsymbol{k}_0 + \boldsymbol{k}_1 s\|^2 = r^2,$$

with

$$\begin{aligned}\boldsymbol{k}_0 &= \left[\boldsymbol{g}_0 - \boldsymbol{x}_0 - \boldsymbol{\Omega} \cdot (\boldsymbol{g}_0 - \boldsymbol{x}_0)\, \boldsymbol{\Omega}\right], \\ \boldsymbol{k}_1 &= \left[\boldsymbol{g}_1 - (\boldsymbol{\Omega} \cdot \boldsymbol{g}_1)\, \boldsymbol{\Omega}\right].\end{aligned}$$

Here $\boldsymbol{k}_0$ represents the vector rejection of $\boldsymbol{g}_0 - \boldsymbol{x}_0$ onto $\boldsymbol{\Omega}$, or the part of the vector connecting the midpoint of the cylinder to the position of the particle that is perpendicular to the cylinder axis. $\boldsymbol{k}_1$ is the same thing, except for $\boldsymbol{g}_1$, the direction of the particle. The equation can further simplify to

$$\begin{aligned}r^2 &= (\boldsymbol{k}_0 + \boldsymbol{k}_1 s) \cdot (\boldsymbol{k}_0 + \boldsymbol{k}_1 s) \\ &= \boldsymbol{k}_0 \cdot \boldsymbol{k}_0 + 2\boldsymbol{k}_0 \cdot \boldsymbol{k}_1 s + \boldsymbol{k}_1 \cdot \boldsymbol{k}_1 s^2.\end{aligned}$$

Defining

$$\begin{aligned}\ell_0 &= \boldsymbol{k}_0 \cdot \boldsymbol{k}_0 - r^2, \\ \ell_1 &= \boldsymbol{k}_0 \cdot \boldsymbol{k}_1, \\ \ell_2 &= \boldsymbol{k}_1 \cdot \boldsymbol{k}_1,\end{aligned}$$

the solution to this equation is

$$s = \frac{-\ell_1 \pm \sqrt{\ell_1^2 - \ell_0 \ell_2}}{\ell_2},$$

which is the distance to collision of the particle with the cylinder. Moving the particle ahead by this distance will move it to the site of intersection. If $l_2 = 0$, the particle continues along the axis of the line forever. If

$$\ell_1^2 - \ell_0 \ell_2 < 0,$$

there are no intersections.

To find the relationship between a cylinder and a particle, the equation is the same as before but with $\boldsymbol{k}_1 = \boldsymbol{0}$, which gives

$$\boldsymbol{k}_0 \cdot \boldsymbol{k}_0 = r^2,$$

or

$$\ell_0 \begin{cases} > 0, & \text{outside,} \\ < 0, & \text{inside,} \\ = 0, & \text{coincident.} \end{cases}$$

The normal direction of a cylinder at a point $\boldsymbol{g}_0$ can be found by normalizing the $\boldsymbol{k}_0$ vector,

$$\hat{\boldsymbol{n}} = \frac{\boldsymbol{k}_0}{\|\boldsymbol{k}_0\|}.$$

16.1.3 Sphere

The equation of a sphere is

$$\|\boldsymbol{x} - \boldsymbol{x}_0\|^2 = r^2, \tag{108}$$

which using the same

$$\boldsymbol{x}_p(s) = \boldsymbol{g}_0 + \boldsymbol{g}_1 s \tag{109}$$

as before gives

$$\|\boldsymbol{g}_0 + \boldsymbol{g}_1 s - \boldsymbol{x}_0\|^2 = r^2.$$

Letting

$$\begin{aligned}\boldsymbol{k}_0 &= \boldsymbol{g}_0 - \boldsymbol{x}_0,\\ \boldsymbol{k}_1 &= \boldsymbol{g}_1,\end{aligned}$$

the results from the cylinder follow exactly. The difference is that

$$\ell_2 = \boldsymbol{g}_1 \cdot \boldsymbol{g}_1 = 1,$$

so that the equation can be simplified to

$$s = -\ell_1 \pm \sqrt{\ell_1^2 - \ell_0},$$

with

$$\begin{aligned}\ell_0 &= \boldsymbol{k}_0 \cdot \boldsymbol{k}_0 - r^2,\\ \ell_1 &= \boldsymbol{k}_0 \cdot \boldsymbol{k}_1.\end{aligned}$$

To check if a particle is inside of the problem, use

$$\ell_0 \begin{cases} > 0, & \text{outside},\\ < 0, & \text{inside},\\ = 0, & \text{coincident},\end{cases}$$

as before. The normal direction of a cylinder at point $\boldsymbol{g}_0$ is

$$\hat{n} = \frac{\boldsymbol{k}_0}{\|\boldsymbol{k}_0\|}.$$

Part VII
Tests

17 Utilities

17.1 Indexing

The indexing test "tst_indexing" tests whether the subscript to index and index to subscript functions work appropriately to restore a given subscript after converting it to the index and back.

17.2 Integration

17.3 Linear algebra

This tests the analytic linear solves against a Trilinos solve. A random matrix $\boldsymbol{A}$ and vector $\boldsymbol{b}$ are created, after which the solution is performed using each of the analytic solves and the Trilinos solution to get the vector $\boldsymbol{x}$. If the L_∞ difference between these two vectors is less than the tolerance, the test is passed.

17.4 Math functions

17.4.1 Factorial

The factorial test compares the analytic value of 12! with a calculated value.

17.4.2 Legendre polynomial

17.4.3 Spherical harmonics

17.5 Quadrature

17.5.1 Gaussian 2D

17.5.2 Double Gaussian 2D

17.5.3 Boundary Gaussian 2D

17.6 Sparse storage

17.7 Trilinos

17.8 Vector functions

Tests vector functions against analytic results.

18 Angular discretization

18.1 Gauss-Legendre

18.2 LDFE

19 Solid geometry

20 Spatial discretization

21 Operator

22 Transport

References

[1] J.S. WARSA, T.A WAREING, J.E. MOREL, "Krylov Iterative Methods and the Degraded Effectiveness of Diffusion Synthetic Acceleration for Multidimensional S_N Calculations in Problems with Material Discontinuities," *Nucl. Sci. Eng.*, **147**(3), 218-248 (2004).

[2] W. CHEN, Z. FU, C. CHEN, *Recent Advances in Radial Basis Function Collocation Methods*, Springer (2014).